Stratifying elicited antibody dynamics after two doses of SARS-CoV-2 vaccine in a community-based cohort in Fukushima, Japan

AUTHORS:

Naotoshi Nakamura[1,†], Yurie Kobashi[2,3,†], Kwang Su Kim[1,4,5,†], Yuta Tani[6], Yuzo Shimazu[2], Tianchen Zhao[2], Yoshitaka Nishikawa[3], Fumiya Omata[3], Moe Kawashima[2], Makoto Yoshida[6], Toshiki Abe[2], Yoshika Saito[6], Yuki Senoo[6], Saori Nonaka[2], Morihito Takita[2], Chika Yamamoto[2], Takeshi Kawamura[7,8], Akira Sugiyama[7], Aya Nakayama[7], Yudai Kaneko[8,9], Hyeongki Park[1], Yong Dam Jeong[1,5], Daiki Tatematsu[1], Marwa Akao[1], Yoshitaka Sato[10], Shoya Iwanami[1], Yasuhisa Fujita[1], Masatoshi Wakui[11], Kazuyuki Aihara[12], Tatsuhiko Kodama[8], Kenji Shibuya[13,14], Shingo Iwami[1,15,16,17,18,19,‡,*] and Masaharu Tsubokura[2,3,6,20,‡,*]

AFFILIATIONS:

[1]interdisciplinary Biology Laboratory (iBLab), Division of Natural Science, Graduate School of Science, Nagoya University, Nagoya, Japan. [2]Department of Radiation Health Management, Fukushima Medical University School of Medicine, Fukushima, Japan. [3]Department of General Internal Medicine, Hirata Central Hospital, Fukushima, Japan. [4]Department of Science System Simulation, Pukyong National University, Busan, South Korea. [5]Department of Mathematics, Pusan National University, Busan, South Korea. [6]Medical Governance Research Institute, Tokyo, Japan. [7]Proteomics Laboratory, Isotope Science Center, The University of Tokyo, Tokyo, Japan. [8]Laboratory for Systems Biology and Medicine, Research Center for Advanced Science and Technology, The University of Tokyo, Tokyo, Japan. [9]Medical & Biological Laboratories Co., Ltd, Tokyo, Japan. [10]Department of Virology, Nagoya University Graduate School of Medicine, Nagoya, Japan. [11]Department of Laboratory Medicine, Keio University School of Medicine, Tokyo, Japan. [12]International Research Center for Neurointelligence, The University of Tokyo Institutes for Advanced Study, The University of Tokyo, Tokyo, Japan. [13]Soma Medical Center of vaccination for COVID-19, Fukushima, Japan. [14]Tokyo Foundation for Policy Research, Tokyo, Japan. [15]Institute of Mathematics for Industry, Kyushu University, Fukuoka, Japan. [16]Institute

for the Advanced Study of Human Biology (ASHBi), Kyoto University, Kyoto, Japan. [17]Interdisciplinary Theoretical and Mathematical Sciences Program (iTHEMS), RIKEN, Saitama, Japan. [18]NEXT-Ganken Program, Japanese Foundation for Cancer Research (JFCR), Tokyo, Japan. [19]Science Groove Inc., Fukuoka, Japan. [20]Minamisoma Municipal General Hospital, Fukushima, Japan.

†,‡ These authors contributed equally to this study.

*To whom correspondence may be addressed.
Email: iwami.iblab@bio.nagoya-u.ac.jp (S.I.) and tsubo-m@fmu.ac.jp (M.T.).

Abstract

Recent studies have provided insights into the effect of vaccine boosters on recall immunity. Given the limited global supply of COVID-19 vaccines, identifying vulnerable populations with lower sustained vaccine-elicited antibody titers is important for targeting individuals for booster vaccinations. Here we investigated longitudinal data in a cohort of 2,526 people in Fukushima, Japan, from April 2021 to December 2021. Antibody titers following two doses of a COVID-19 vaccine were repeatedly monitored and information on lifestyle habits, comorbidities, adverse reactions, and medication use was collected. Using mathematical modeling and machine learning, we stratified the time-course patterns of antibody titers and identified vulnerable populations with low sustained antibody titers. Moreover, we showed that only 5.7% of the participants in our cohort were part of the “durable” population with high sustained antibody titers, which suggests that this durable population might be overlooked in small cohorts. We also found large variation in antibody waning within our cohort. There is a potential usefulness of our approach for identifying the neglected vulnerable population.

Main Text

Primary two-dose coronavirus disease 2019 (COVID-19) vaccination leads to rapid immunity, providing protection against severe acute respiratory syndrome coronavirus 2 (SARS-CoV-2) infection[1]. Although COVID-19 vaccines still offer good protection against severe disease and death for months after the second dose owing to the durability of immunity[2-4], the waning of vaccine efficacy has become a major concern in the era of "living with COVID-19"[5-9]. The rapid decline in vaccine-elicited antibodies results in breakthrough infections and adverse health outcomes caused by emerging variants of concern (VOCs), including the Beta, Delta, and Omicron variants[10-13]. Additional third and fourth doses of vaccine induce a high-level antibody response against VOCs[13-17], implying a need for additional booster vaccinations as a future pandemic exit strategy[18-20]. Few studies, however, have quantitatively stratified and assessed the variation in waning of antibody titers at both the population and individual level in a community-based large cohort.

At the population level, it is well known that the older a person is, the faster their protection weakens after the second vaccination[7,8], and that people with underlying medical conditions tend to induce an insufficient antibody response[8,21]. These populations are generally the highest priority group for booster vaccinations. There is, however, large variation in the vaccine-elicited antibody response at the individual level, even within the same age group[6-8,15,21,22]. Assessing the factors that affect such variations will shed further light on our understanding of waning of protection and identify potentially vulnerable populations that may be a priority for booster vaccination[8,21]. In the long-run, personalized vaccination will be required, because continuous vaccinations after the third dose to the whole population may be neither sustainable nor feasible globally. One approach to assess variation within the same group of people is the stratified analysis of time-dependent vaccine-elicited antibody dynamics.

Although the mean time-dependent vaccine efficacy for symptomatic and severe SARS-CoV-2 infections has been assessed through cross-sectional and longitudinal studies at the

population level[2,3], many relevant aspects of the individual-level time course of antibody dynamics and the variations in individual-level dynamics are not well understood. In this study, we collected longitudinal datasets on individual antibody responses, together with personal information including lifestyle habits, comorbidities, adverse reactions, and medication use, from more than 2,526 individuals of a community-based cohort in Fukushima, Japan. Taking advantage of this unique cohort and using mathematical modeling and machine-learning approaches, we stratified the elicited immune response after two doses of a COVID-19 vaccine by reconstructing individual antibody dynamics. Furthermore, we explored the factors associated with the durability of vaccine response. Our aim was to understand individual-level variation in vaccine-elicited immune responses at the time of booster vaccinations and to inform long-term COVID-19 vaccination strategies.

Results

The Fukushima vaccination cohort

This study was conducted from April 2021 to December 2021 in Fukushima, Japan. Our vaccination cohort consisted of participants from a primarily rural area where COVID-19 prevalence was relatively low: Soma City, Minami Soma City, and Hirata village (**Fig 1A**). The participants included health care workers, frontline workers, administrative officers, general residents, and residents of long-term care facilities. In total, 2,526 participants who had been vaccinated with the Pfizer BNT162b2 or Moderna mRNA-1273 vaccine were recruited, and 2,159 participants were included in the final data analysis, respectively (see **Fig 1B** and **Methods** in details). The age and sex distributions of the participants are shown in **Fig 1C**, and the sample characteristics and information on adverse vaccine events stratified by age are provided in **Extended Data Table 1**. A portion of this cohort was described previously for the time period extending to 6 months after the first dose of mRNA vaccine[23,24].

Here we investigated antibody titers in the Fukushima cohort in individuals sampled longitudinally (serum was collected at 2 or 3 different timepoints) for around 4 to 9 months after the second primary dose of mRNA vaccine (see **Fig 1DE** for details). Notably, the number of SARS-CoV-2 infections in this rural area was extremely low (**Fig 1E**), so that we could minimize the influence of breakthrough natural infections. The Fukushima cohort, which is large enough and with a long study period (**Fig 1F**), is an ideal longitudinal cohort for quantifying and stratifying vaccine-elicited antibody dynamics (**Supplementary Note 1** and **Supplementary Table 1**). In particular, compared with the largest cohort of more than 3,900 participants from Israel,[6] the Fukushima cohort is community-based, includes non-health workers, has very few dropouts among more than 2,000 identical individuals who were consecutively sampled (only 3.3%), includes all necessary information for all participants, and includes measures of several modalities of antibody titers including neutralizing activity (**Supplementary Table 2**).

We performed chemiluminescent immunoassay (CLIA) to measure antibody titers as a measure of humoral immune status after the first COVID-19 vaccination (i.e., a total of 5195

IgG(S), 5195 neutralization activity, and 4969 IgG(N) assays were performed) (**Methods**). **Fig 1G** shows the overall profile of IgG(S) and neutralization activity in this study. We investigated longitudinal data for IgG(S) in the same individuals because IgG(S) covers a wider range of antibody responses and is more sensitive than neutralization activity. In fact, these two measurements are highly correlated with each other (correlation coefficient of 0.93) (**Extended Data Fig 1AB**), and previous studies showed that neutralizing antibody and IgG(S) titers correlate with vaccine-mediated protection, even against VOCs (i.e., vaccine efficacy)[1-3]. This is because vaccines containing the original Wuhan virus spike protein induce variant-reactive memory B cells targeting multiple different VOCs, including the Omicron variant[15].

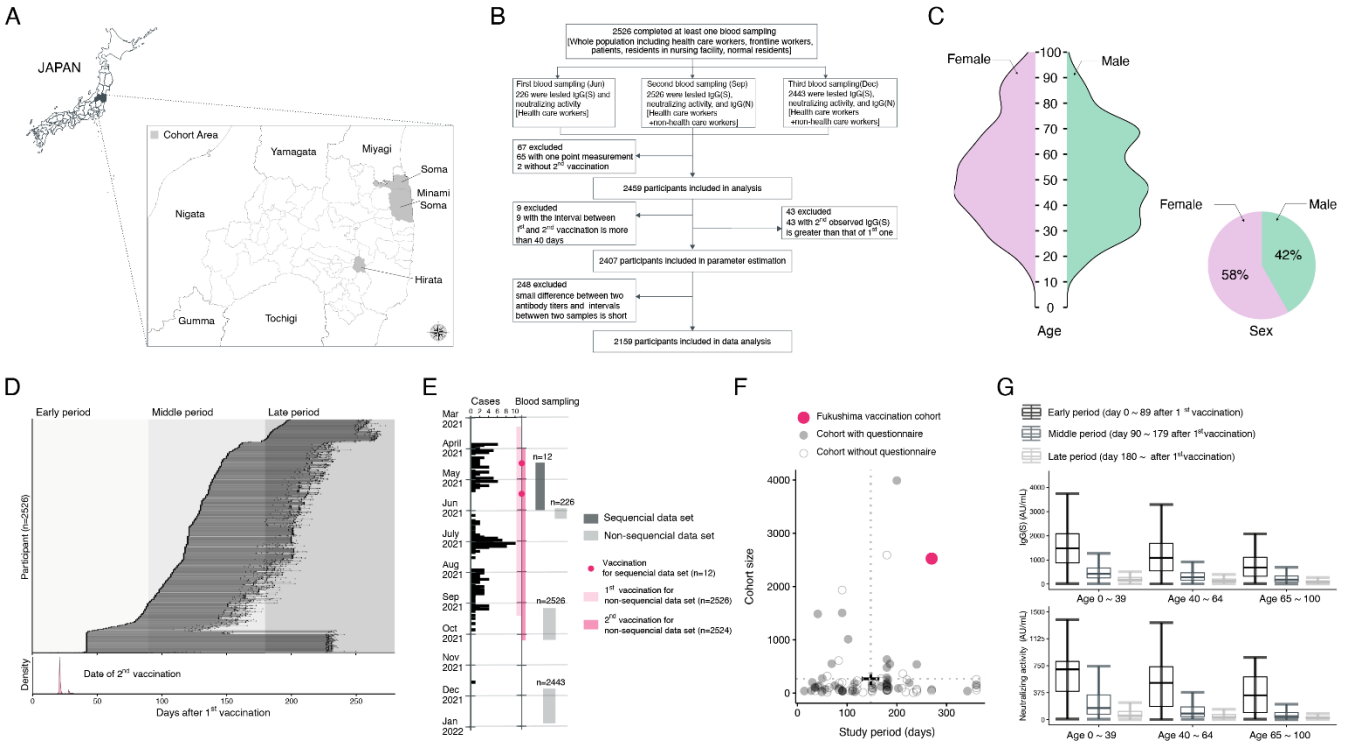

Figure 1 | Characteristics of the Fukushima vaccination cohort: (A) Locations of Soma city, Minami Soma city, and Hirata village in Fukushima prefecture are described. **(B)** Flowchart of the vaccination cohort along with the number of participants, testing, and inclusion criteria for our analysis are described. **(C)** Age and sex distributions in the cohort are shown. **(D)** Timeline of sample collection for each cohort participant (N=2,526 participants, 5195 total samples) is described. The timings of blood samplings are indicated in black circles. Shaded areas indicate early (<89 days), middle (90-179 days), and late (>180 days) time periods after the first vaccination. Dates for the second vaccination are shown as the distributions in the bottom panel. **(E)** Vaccination and blood sampling periods in the cohort along with the number of COVID-19 cases (i.e., cases) in Soma city, Minami Soma city, and Hirata village[48,49] are shown. **(F)** Distribution of the study periods and the number of participants (i.e., cohort size) of previously reported cohorts extracted by literature review (**Supplementary Note 1**) are plotted along with the Fukushima vaccination cohort (the red mark). The closed and open marks correspond to cohorts with and without questionnaire data. The origin of coordinates corresponds to the median of the period and number of the cohorts, and the whiskers indicate corresponding standard derivations. **(G)** Longitudinal IgG(S) and neutralizing activity measured by CLIA are separately plotted by time after the first vaccination and age.

Stratification of vaccine-elicited time-course antibody dynamics

We developed a mathematical model describing the vaccine-elicited antibody dynamics to evaluate the impact of primary two-dose COVID-19 vaccination on rapid immunity at the individual level and reconstructed the best-fit antibody titer curves of 2,407 participants in the Fukushima cohort (details are provided in the **Methods**). We then performed an unsupervised clustering analysis using a random forest dissimilarity to stratify the time-course patterns of antibody dynamics into six groups (i.e., G1 to G6) (details in **Supplementary Note 2**). **Fig 2A** represents a two-dimensional Uniform Manifold Approximation and Projection (UMAP) embedding of these six groups, which clearly shows that G5 and G6 are separated from the other groups. Using a different color for each group, we also plotted the reconstructed individual antibody dynamics after 25 days after the first vaccination as shown in **Fig 2B** (see also **Extended Data Fig 2D**). The projected time course of each group showed that sustained antibody titers remained high among individuals in G1 (i.e., the “rich” responder group), whereas those in G5 and G6 were low (i.e., “poor” responders) (**Fig 2C**). We classified G1 as a “durable” population and G5/G6 as a “vulnerable” population in our analysis. In contrast, individuals in G2, G3, and G4 showed intermediate dynamics. Note that most individuals in the Fukushima cohort had no history of natural infection (i.e., only 1.07%).

Next, we investigated the age dependency of the 6 groups (**Fig 2D**): G1/G2, G3/G4, and G5/G6 consisted mainly of people aged 0 to 39 years (young), 40 to 64 years (middle age) and 65 to 100 years (old), respectively. Most individuals were stratified into G3 or G2, the representative population of the Fukushima cohort (**Fig 2E**). Although the age distributions of G1/G2 and G3/G4 were similar, individuals in G2 and G4 showed a relatively rapid decay in antibody response after the second dose compared with those in G1 and G3, respectively (**Extended Data Fig 2D**).

The longitudinal IgG(S) and neutralizing activity measured by CLIA are separately plotted into three different periods (i.e., 0-89, 90-179, ≥180 days) by taking into account the stratified groups in **Fig 2F**. Both IgG(S) and neutralizing activity decreased as age increased and time

passed. More precise predictions (i.e., at a specific date at an individual level rather than during a specific period at a population level) were made possible with our reconstructed individual-level antibody dynamics (**Fig 2G**).

To further evaluate the vaccine-elicited immunity, we calculated the fraction of individuals with antibody titers of IgG(S) below set thresholds (i.e., 10 and 200 arbitrary unit/mL [AU/mL]) (**Fig 2H**). As reported in the study by Nakano et al.[25], 10 AU/mL is a clear threshold for unvaccinated individuals, meaning that individuals showing titers less than this threshold have no vaccine efficacy at all. In contrast, so far, there are no clear thresholds for quantifying vaccine efficacy, as intensively discussed in Cromer et al.[2] and Khoury et al.[3]. Here we used the value of 200 AU/mL as an indicator for the efficacy threshold, because more than 80% of vaccinated persons maintained their antibody titers above 200 AU/mL during the early period (i.e., for at most 3 months after the first vaccination) regardless of group in our cohort (see the top-left panel in **Fig 2F**). Our simulations showed that most of the durable population (i.e., G1) maintained their vaccine efficacy for at least 8 months, and furthermore, around 13% of them still did not show a loss of vaccine efficacy for 1 year after the first vaccination (**Fig 2H**). On the other hand, the vulnerable populations (i.e., G5/G6) showed a low induction of antibody titers after the second dose and rapid decay in efficacy; approximately 50% of them had very low antibody titers after 1 year, which were comparable to those in unvaccinated persons. Individuals in G4 showed a high initial induction of antibody titers after the second dose but a rapid decay; approximately 95% of them showed a loss of vaccine efficacy after 1 year.

For our sensitivity analysis, we used the threshold of 80 AU/mL, which corresponds to "strong positive" as defined in the Mount Sinai Health System[26] and obtained the same conclusions (e.g., **Supplementary Fig 1A** for 80 AU/mL).

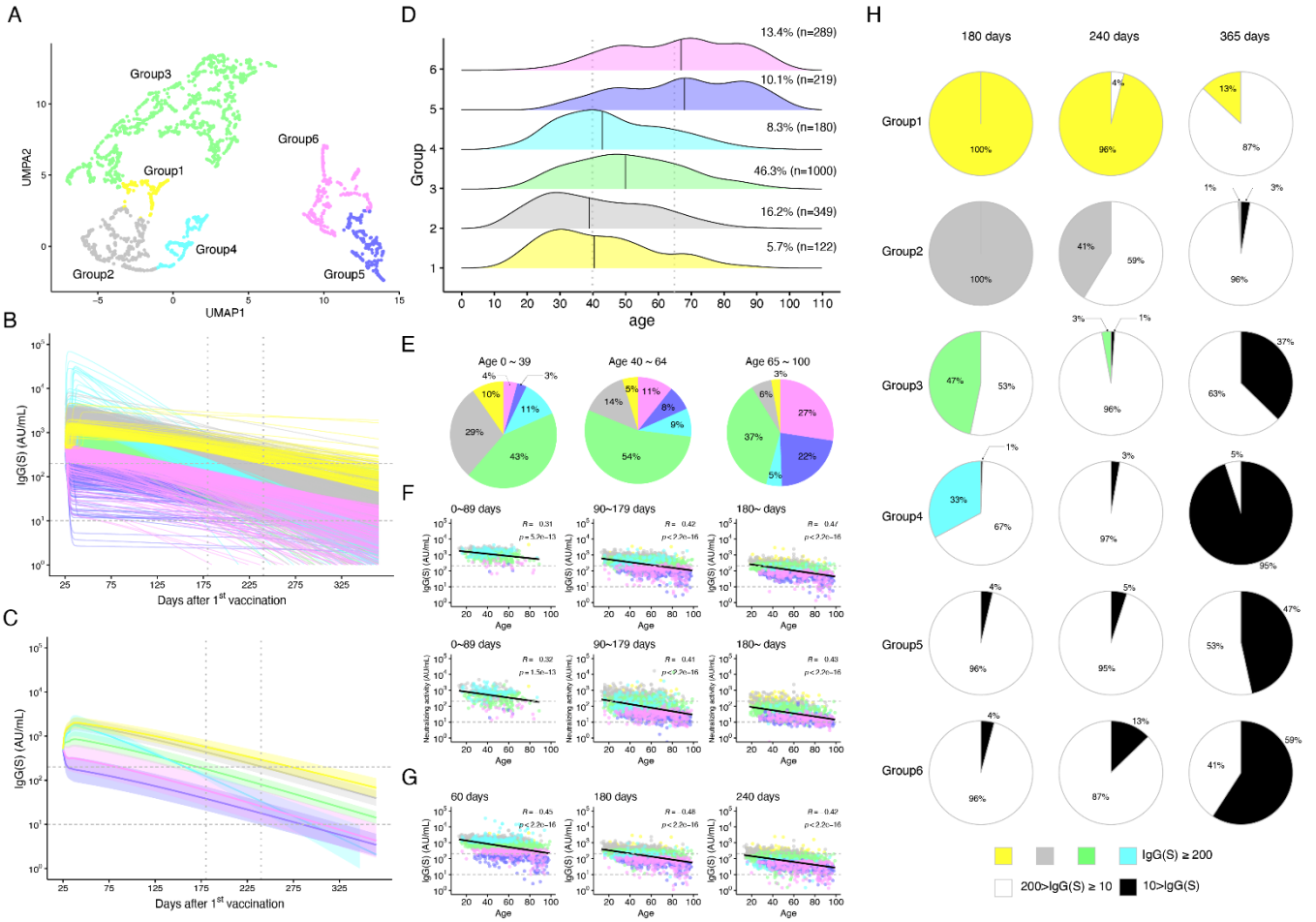

Figure 2 | Stratification of vaccine-elicited antibody response: (A) UMAP of stratified antibody responses to mRNA vaccination based on the extracted features from the reconstructed individual-level antibody dynamics are shown. Data points represent individual participants and are colored according to group (i.e., G1 to G6). **(B)** The reconstructed individual antibody dynamics after 25 days after the first vaccination in each group are shown. **(C)** The time-course patterns highlighted by Partial Least-Squares Discriminant Analysis (PLS-DA), which discriminates each group from the others, are shown. The individual dynamics after 25 days after the first vaccination were projected onto the direction of the first latent variable. The horizontal dashed lines at 200 and 10 AU/mL correspond to the thresholds of "vaccine efficacy" and unvaccinated persons, respectively. The vertical dotted lines represent 180 and 240 days after the first vaccination. **(D)** Age distribution in each group along with its fraction (%) and the number of individuals (n) is shown. **(E)** Group distribution by age (i.e., 0-39, 40-64, 65-100) is plotted in pie charts. **(F)** Measured IgG(S) and neutralizing activity in each group are plotted in the early, middle, and late period. **(G)** Simulated IgG(S) titers from reconstructed individual-level antibody dynamics at 60, 180, and 240 days after the first vaccinations are plotted. **(H)** Fraction of individuals with antibody titers <10, 10-200, and 200 < AU/mL in each group at 180, 240, and 365 days are plotted as black, white, and group color, respectively, in pie charts. All correlations were calculated as Pearson correlation coefficients.

Characterizing vulnerable and durable populations

Multiple factors, including underlying medical conditions, drug history, and immune competency, may contribute to the stratification of the study population. For example, there was substantial variation in sustained immunity within the same age group (e.g., age distributions in both the durable and vulnerable populations were wide), and about 7% of the vulnerable population in G5/G6 were young individuals (0-39 years of age) (**Fig 2E**).

To further characterize each stratified group, we trained a random forest classifier to predict the group from the sample characteristics of 2159 individuals in the Fukushima cohort (see **Extended Data Table 1**), and obtained ROC-AUCs of 64.4%, 69.3%, and 70.9% for predicting G1 (the durable population), G2, and G1/G2, respectively (**Fig 3A**). Analysis of the feature importance suggested that adverse reactions (e.g., headache and joint pain) were significant predictors common to both G1 and G2 (**Fig 3C**). On the other hand, we achieved ROC-AUCs of 78.0%, 75.1%, and 80.8% for predicting G5, G6, and G5/G6 (the vulnerable populations), respectively (**Fig 3B**). Various factors including age, the interval between the two doses, comorbidities, and medication use were listed as the significant predictors of G5 and/or G6 (**Fig 3D**). This finding was consistent with the results of our literature review (see **Supplementary Table 3**). We were not able to achieve a high ROC-AUC for predicting G3 and G4, the groups into which the majority of our cohort participants fell (see **Extended Data Fig 3A** and **Discussion**).

Furthermore, when the classifier for G5/G6 was trained after the population was stratified according to age (i.e., 0-39 [young], 40-64 [middle age], and 65-100 [old]), the ROC-AUCs were 69.3%, 68.7%, and 70.1%, respectively (see **Extended Data Fig 3B**). Our analysis of the feature importance suggested that medication use (e.g., anti-cancer agents, steroids, and immunosuppressants) was a significant predictor for young people, whereas alcohol consumption and smoking played an additional role for middle-aged persons (**Fig 3E**). The detailed inter-relationship of the various features described in **Fig 3F** and **Extended Data Fig 3C** are explained in **Supplementary Note 3**.

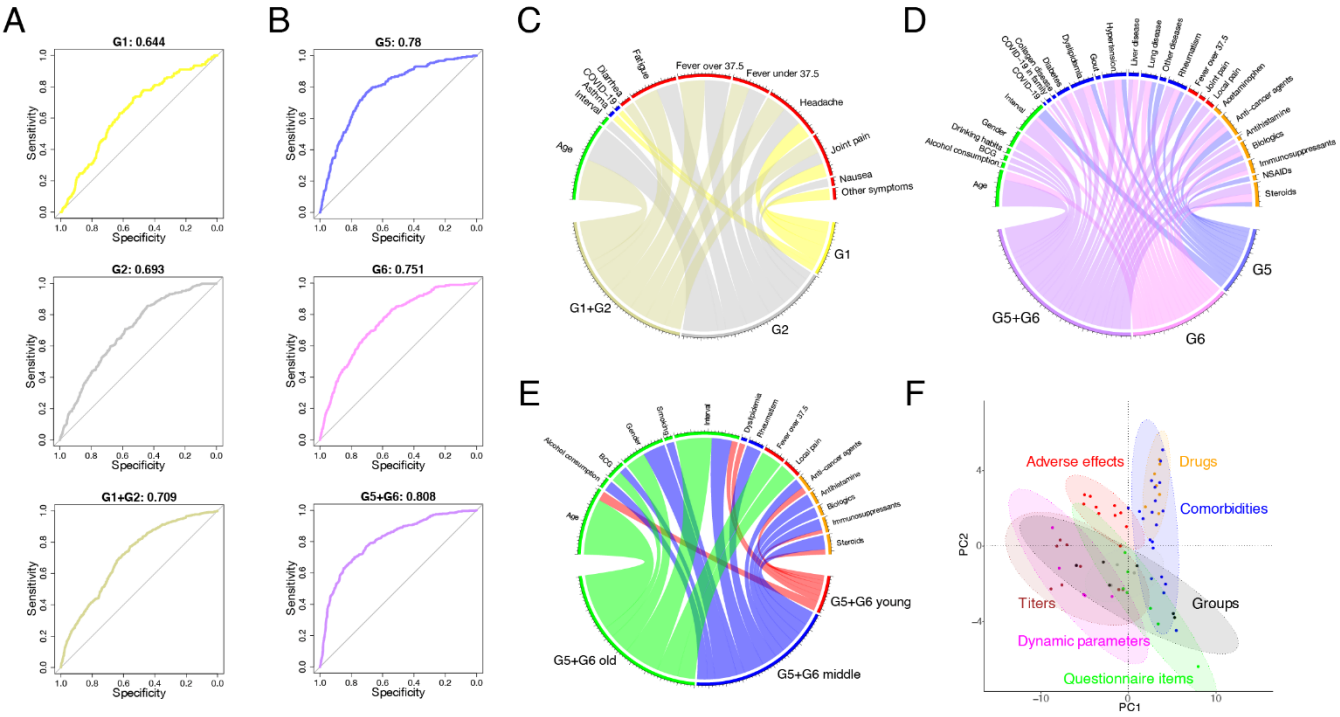

Figure 3 | Characterization of vulnerable and durable populations: (A) and **(B)** show the ROC curves of random forest classifiers trained on predicting either G1 (durable population); G2 or G1/G2; and G5, G6, or G5/G6 (vulnerable population), respectively. The corresponding AUC value of each ROC curve is calculated on the top of each panel. **(C)** and **(D)** show the most predictive features (feature importance) of G1, G2, and G1/G2 and G5, G6, and G5/G6 as Chord diagrams, respectively. Each feature is represented by a fragment on the outer part of the circular layout. The size of the arc from a group to a feature is proportional to its importance as measured by mean decrease in accuracy. Features with $p < 0.05$ are displayed. **(E)** The most predictive features of G5/G6 in young, middle-aged, and old populations are calculated and shown as a Chord diagram. Features with $p < 0.05$ are displayed. **(F)** Principal component analysis of various features is shown. The colored ellipses represent 90% data ellipses drawn for each category.

Predicted effect of booster vaccination on stratified antibody dynamics

Several studies have reported that booster doses after the primary two-dose vaccination rapidly increase antibody titers to a high level, and that these booster-elicited antibody responses induce substantial neutralization against VOCs, including the Omicron variant[15-17]. However, it remains unclear how booster vaccinations shape the induction of antibody response depending on the second-dose, vaccine-elicited antibody dynamics (i.e., the time-dependent vaccine-elicited antibody history). Despite the current limited vaccine supply and large variation even within the same stratified group, the priority for booster vaccines at the “individual level” of immunity and the effect of boosters on “population-level” immunity are not well understood.

Assuming similar immune kinetics of the second-dose, vaccine-elicited antibody dynamics, we modeled the elicited antibody responses on each group over the first year after the booster vaccination at 8 months after the first vaccination (**Fig 4A**). Consistent with the current booster vaccination studies[13,14,16-20,27], our simulations showed a rapid and high induction of antibody responses regardless of group. Moreover, our simulation supported that a third-dose vaccination booster protects against VOCs in a wide range of populations. In contrast, 35% and 9% of G5 and G6, respectively, at 1 month after booster vaccination showed limited induction (i.e., less than 200 AU/mL) (see **Fig 4B**). We also confirmed a similar trend for booster vaccination at 1 year (**Extended Data Fig 4A**), and at the threshold of 80 AU/mL at 8 months (**Supplementary Fig 1B**). The existence of these vulnerable populations may explain the considerable variability in booster-elicited antibody responses observed in several cohort studies[6-8,15]. Targeting individuals in G5/G6 for booster vaccination is expected to provide protection from breakthrough infection.

Next, taking advantage of our stratification, we further evaluated the effect of booster vaccination on population-level immunity. Here we assumed a hypothetical cohort of 10,000 individuals, adjusted for age and sex distributions according to population estimates in Japan as of 1 July 2021 by the Statistics Bureau of Japan, Ministry of Internal Affairs and Communications[28]

(**Fig 4C**). We excluded populations aged less than 12 years in our simulations to reflect the age threshold of the cohort.

First, we simulated the fraction of individuals with antibody titers below the thresholds (i.e., 10 and 200 AU/mL) when all individuals received a booster vaccine (i.e., 100% booster coverage) at different time periods (8 and 12 months after the first vaccination) in **Extended Data Fig 4BC**. As expected, 100% booster coverage effectively increases and recovers their immune responses regardless of timing compared with the no booster scenario. Since 100% booster coverage is too optimistic given the limited vaccine supply, we next applied more realistic booster strategies: 20% and 50% coverage of booster vaccinations (**Fig 4DE** and **Extended Data Fig 4DE**). We compared the booster vaccinations to 2,000 individuals (i.e., 20% of the total 10,000 population: 20% booster vaccination) in G1/G2 (green curve: the durable population and others), G5/G6 (red curve: the vulnerable population), and randomly sampled groups (blue curve) in **Fig 4DE**. Although small differences were observed for the fraction with the threshold of 200 AU/mL (**Fig 4D**), the booster vaccinations provided similar benefit to population-level immunity regardless of population clusters. Similar trends in 50% booster coverage are shown in **Extended Data Fig 4DE**. Here we again stress that the same conclusions are obtained with different thresholds instead of 200 AU/mL (e.g., **Supplementary Fig 1CDE** for 80 AU/mL). Considering the relative benefit of booster vaccinations at the individual level, our identified vulnerable population is a candidate for priority booster vaccination under the limited vaccine supply (see **Discussion**).

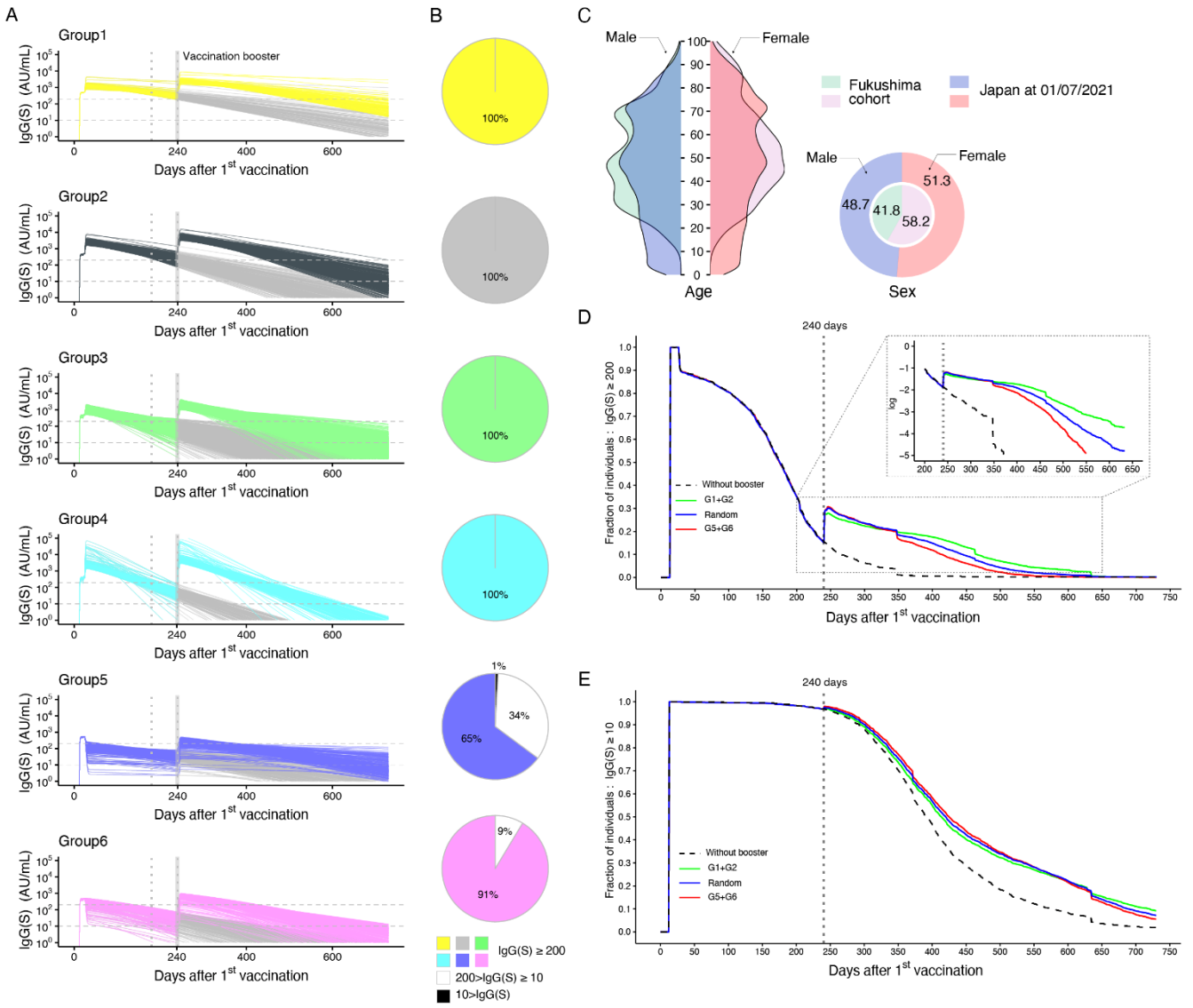

Figure 4 | Simulating booster vaccines: (A) Predicted individual elicited antibody responses for each group over the first year after booster vaccination at 8 months after the first vaccination are shown. The horizontal dashed and vertical dotted lines correspond to 200 and 10 AU/mL and at 180 and 240 days after the first vaccination, respectively. **(B)** Fraction of individuals with antibody titers of <10, 10-200, and 200 < AU/mL in each group at 1 month after booster vaccination are plotted as black, white, and group color, respectively, in pie charts. **(C)** Age and sex distributions of a hypothetical cohort adjusted via population estimates in Japan are shown along with those in the Fukushima vaccination cohort. **(D)** and **(E)** show the time-dependent fractions of individuals with antibody titers above 200 and 10 AU/mL with (i.e., colored curves) and without (i.e., black dashed curve) 20% booster vaccination at 240 days after the first vaccination, respectively. The green, blue, and red curves correspond to the booster vaccination targeting individuals randomly sampled from G1/G2, G1-G6, and G5/G6, respectively. Enlarged view of the dotted box in **(D)** shows the fraction plotted in log-scale.

Discussion

As of May 6, 2022, there were 266 COVID-19 vaccine candidates undergoing phase 1/2 clinical trials and 124 candidates in phase 3 clinical trials (ClinicalTrials.gov). However, it is expected to take more time until second-generation vaccines that block transmission of Omicron and other novel virus variants with a much higher probability than current ones are available around the world. We still need to use the current first-generation vaccines as vaccine boosters. Therefore, determining the priority for booster vaccines in the vulnerable population is an important public health concern given a limited global supply of vaccines[13-20].

In this study, we aimed to understand the individual-level variation in vaccine-elicited immune responses at the time of booster vaccinations and the effect of booster vaccination. Only 1.07% of our cohort of individuals had a history of natural infection; thus, the influence of natural infection was minimal in the present study. We repeatedly assessed and monitored antibody titers following two doses of a SARS-CoV-2 vaccine in the unique Fukushima cohort of 2,526 individuals.

Previous studies generally investigated differences in vaccine-elicited antibody responses after stratification of the population according to variables including age, sex, lifestyle habits, comorbidities, adverse reactions, and medication use (i.e., in “given” groups). For example, Levin and colleagues explored differences in antibody responses according to age, sex, and immunesupression[8]. Ward and colleagues also showed that antibody responses are significantly decreased in individuals with diabetes, obesity, smoking habits, cancer, immunosuppression, or neurological conditions after adjustment for age and sex[29]. It is well known that active cytotoxic chemotherapy and specific comorbidities such as kidney disease, hypertension, and heart disease significantly affect antibody responses[22,30-32]. Importantly, in our cohort, we identified six groups with different antibody responses by using a combined approach with process-based mathematical modeling and data-driven analysis (i.e., without determining these “given” groups in advance as mentioned above). In particular, we found that G1 mainly consisted of participants aged 0 to 39 years who were part of the durable population (i.e., those who were “rich” responders

showing high sustained antibody titers), whereas G5/G6 consisted of participants aged 65 to 100 years who were part of the vulnerable population (that is, those who were “poor” responders showing low sustained antibody titers). Our study showed that more than 10% of the durable population maintained their IgG(S) titers above 200 AU/mL for 1 year after the first vaccination, whereas approximately 50% of the vulnerable population could not maintain their antibody titers above 10 AU/mL after 1 year (i.e., they completely lost their vaccine efficacy).

An important question is how we maintain both individual- and population-level immunity through booster vaccinations. Although T and B cell responses may contribute to protection from symptomatic and severe infections[4,12,27,33], recent studies have shown that vaccine efficacy is strongly linked to the elicited antibody responses, meaning that sustained high antibody titers above a certain threshold are crucial[2,3,34]. The present study showed that vulnerable populations (i.e., G5/G6) include individuals who are not necessarily older adults nor with high-risk conditions. In fact 5.5% of G5/G6 were young adults who did not have any underlying medical conditions but reported at least one adverse reaction. Although there is no clear consensus for the threshold so far, we found that individuals in G4 maintained high antibody titers induction for months, but their titers rapidly decreased below 200 and 80 AU/mL around 6 and 7 months after the first dose on average, respectively. Because individuals who are classified in G4, G5, and G6 represent those with poor or rapidly decaying vaccine-elicited antibody responses who would not necessarily benefit from the current prioritized booster program on the basis of age and prior medical conditions, it may be important to better understand the large variation in vaccine-induced immunity at the individual level as shown in the present study. Identifying these target individuals and recruiting them to booster vaccinations are important tactics.

Most of the durable population (i.e., G1) will maintain their antibody titers induced by the second dose of mRNA vaccine at high levels at least for 8 months after the first dose, implying that the priority for booster vaccinations is low. Individuals in G1 had no history of natural infection except for one participant. In our study cohort, G1 made up only 5.7% of the cohort, and we only identified these participants because of the large participant size of the Fukushima cohort (over

2,500 individuals). In other words, if the cohort size was in the range of several hundreds, which is the usual size of prior studies made up of health care workers volunteers[30,35-38] (e.g., 93.5% of 93 cohort studies in our literature review had less than 1,000 participants, see **Supplementary Note 1**), these durable individuals might not have been identified and might have been overlooked as outliers (e.g., around 5 individuals in a cohort of 100 individuals). Although the representativeness of the small cohort is unclear (only 61 individuals), preexisting high antibody titers before booster vaccination may limit the extent of antibody boosting (see below)[15].

Our study suggests that booster vaccination of the vulnerable populations of G5/G6 at 80 days after the first vaccination increases antibody titers at both the individual and population level. Booster vaccinations added similar effects to population-level immunity regardless of a population profile under the limited vaccine supply (i.e., 20% and 50% booster coverage) in our simulations. These scenario-based simulations provide novel insights on the timing for booster vaccinations to maintain both individual- and population-level immunity against the emerging and future VOCs.

Overall, our analysis showed a large variation in vaccine-elicited antibody response at the individual level[6-8]. Additional work is required to evaluate how specific antibody neutralizations of VOCs, as quantified by live virus, influence the stratification[13,15,27], and how vaccine-elicited cellular immunity, including B and T cell responses, would explain such variations[12,15]. In particular, we used only the basic demographic information for the characterization of the six groups and are currently collecting additional longitudinal immunologic information, such as cellular immune changes (e.g., memory B cell compartments) and cytokine and chemokine profiles of the vaccinated individuals in our cohort. This will enable us to test and further characterize and understand durability and vulnerability in G1 and G5/G6, respectively[15].

There is an assumption in our mathematical model underlying the vaccine-elicited antibody response: antibodies are simply assumed to be generated from one compartment of B cells including heterogeneous cell populations that produce antibodies. That is, our mathematical model describes the vaccine-elicited antibody responses induced by the average B cell populations. As additional datasets become available on time course and quantitative phenotypic

B cell populations such as short-lived antibody-secreting cells (i.e., plasmablasts), long-lived antibody-secreting cells (i.e., plasma cells), and SARS-CoV-2-specific (class-switched) memory B cells,[9,39] it will be necessary to adjust our mathematical model to more precisely differentiate the antibody dynamics of different B cells. In a recent study with a small sample size, the decay rate of S-specific IgG from its peak to around 6 months after the first dose was similar, but the average decay slowed between 6 and 9 months[15]. Other studies suggest that germinal center B cell responses are critical to maintain the longevity of sustained antibody titers apart from the quick and large antibody production immediately after the second vaccination (or infection)[40-42]. Although this emerging evidence for the heterogeneity of B cell populations implies that the two-compartment model of antibody-secreting cells (i.e., plasmablasts and plasma cells) may better describe IgG(S) dynamics, our mathematical model describes the IgG(S) dynamics of 2,159 individuals (of which 208 individuals had 3 samples collected) at least until around 9 months after the first dose. Our stratification is based on feature engineering but not reconstructed antibody dynamics directly, meaning that the effect of the late-phase dynamics is minimal. However, long-term prediction of antibody dynamics by use of our mathematical model will not be possible.

Important research questions remain: whether people will be classified into the same (or similar) stratified groups after booster vaccination, how the booster vaccine-elicited antibody response will change depending on the interval between the second and third doses, and which group shows low and high neutralization to (emerging) VOCs, for example. The Fukushima cohort is an ideal environment in which to evaluate how immunity, including humoral and cellular responses of durable and vulnerable individuals, is increased by future SARS-CoV-2 infections after the booster vaccination. Taking advantage of our Fukushima cohort, we will further evaluate the impact of booster vaccinations and post-vaccination infections on the identified vulnerable populations[43,44].

METHODS

Ethics statement

The study was approved by the ethics committees of Hirata Central Hospital (number 2021-0611-1) and Fukushima Medical University School of Medicine (number 2021-116). Written informed consent was obtained from all participants individually before the survey.

Participant recruitment and sample collection

The candidates were mainly recruited from Hirata village, Soma city, and Minamisoma city in rural Fukushima prefecture. We conducted sequential blood sampling and non-sequential blood sampling. Twelve health care workers participated in the sequential blood sampling, and their vaccination and blood sampling schedule are shown in **Fig 1E**. A total of 2526 individuals participated in non-sequential blood sampling. Health care workers, frontline workers, and administrative officers from each municipality were intentionally recruited to keep the cohort size large and the dropout rate low. Although most of the health care workers, frontline workers, and administrative officers were under the age of 65, relatively healthy community-dwelling older adults living in the community and in long-term care facilities were also recruited to maintain a wide age range for the cohort. Blood sampling was performed once during each period in June, September, and November 2021, respectively. The first vaccine dose was administered between March 10 and August 20, 2021, and the second dose between March 31 and September 14. The median (interquartile range) interval for the two-dose vaccination was 21 days. A total of 226 health care workers participated in the first blood sampling between May 31 and June 6, 2021. A total of 2526 individuals participated in the second blood sampling between September 8 and October 8, 2021. A total of 2443 individuals participated in third blood sampling between November 21 and December 25, 2021 (**Fig 1E**). Note that the 12 health care workers (described in **Extended Data Fig 5B**) with sequential blood sampling were not included in the non-sequential population of 2526 participants. In conclusion, of the total 2526 participants, those eligible for analysis were those who completed the second vaccination and at least two blood samplings.

Participants whose antibody titer was higher than in the previous blood sampling in non-sequential blood sampling were excluded from the final analysis (**Fig 1B**).

Information on sex, age, daily medication, medical history, date of vaccination, adverse reaction after vaccination, type of vaccination, blood type, bacillus Calmette–Guérin (BCG) vaccine history, smoking habit, and drinking habit was retrieved from the paper-based questionnaire (summarized in **Extended Data Table 1**). All blood sampling was performed at the medical facilities with 8 mL, and serum samples were sent to The University of Tokyo.

SARS-CoV-2-specific antibody measurement

All serological assays were conducted at The University of Tokyo. Specific IgG (i.e., IgG(S)) and neutralizing activity were measured as the humoral immune status after COVID-19 vaccination. Specific IgG antibody titers (IgG(N)) were used to determine past COVID-19 infection status. Chemiluminescent immunoassay with iFlash 3000 (YHLO Biotech, Shenzhen, China) and iFlash-2019-nCoV series (YHLO Biotech, Shenzhen, China) reagents were used in the present study. The threshold value was 10 AU/mL. The measurement range was 2-3500 AU/mL for IgG(S) and 4-800 AU/mL for neutralizing activity. For neutralizing activity, AU/mL×2.4 was used to convert to International Units (IU/mL); for IgG(S), AU/mL×1.0 was used to convert to binding antibody units (BAU/mL). The testing process was as per the official guideline. Quality checks were conducted every day before starting the measurement.

Mathematical modeling of (booster) vaccine-elicited antibody dynamics

We developed a simple but quantitative mathematical model describing the vaccine-elicited antibody dynamics as follows:

$$\frac{dM_i(t)}{dt} = \begin{cases} 0 & (t < \tau_i) \\ -dM_i(t) & (t \geq \tau_i) \end{cases}, \qquad (1)$$

$$\frac{dB(t)}{dt} = P_i(t)\frac{M(t)^m}{K^m + M(t)^m} - \mu B(t)\,, \qquad (2)$$

$$\frac{dA(t)}{dt} = pB(t) - cA(t), \qquad (3)$$

where the variables $M_i(t)$, $B(t)$, and $A(t)$ are the amount of mRNA inoculated by the i-th vaccination, the number of antibody-secreting cells, and the antibody titers at time t, respectively. Parameters τ_i and d represent the timing of the i-th vaccination and the decay rate of mRNA. Note that $\tau_1 = 0$ is assumed for all individuals and $\tau_2 - \tau_1$ corresponds to the interval of the first and second vaccinations. We here considered that D_i is the inoculated dose of mRNA by the i-th vaccination, that is, $M_i(\tau_i) = D_i$ for $i = 1,2, \dots, n$, and $M(t) = \sum_{i=1}^{n} M_i(t)$.

In our mathematical model, one compartment of B cells including heterogeneous cell populations that produce antibodies is assumed, and therefore the product of $P_i(t)$ and $M(t)^m/(M(t)^m + K^m)$ represents the average *de novo* induction of the antibody-secreting cells, that is, the average B cell population dynamics is modeled. Here $P_i(t)$ is a step function defined as $P_i(t) = P_i$ for $\tau_i + \eta_i \leq t < \tau_{i+1} + \eta_{i+1}$, where η_i is the delay of induction of the antibody-secreting cells after the i-th vaccination: otherwise $P_i(t) = 0$. The parameters m, K, and μ correspond to the steepness at which the induction increases with increasing amounts of mRNA (i.e., the hill coefficient), the amount of mRNA satisfying $P_i/2$, and the average decay rate of the antibody-secreting cell compartment, respectively.

For example, after the first vaccination, antigen-specific B cells expand and induce antibody-secreting cells and memory B cells. This rapid immune response regarding expansion and induction is formulated by the function of $P_1 M_1(t)^m/(M_1(t)^m + K^m)$ for $\eta_1 \leq t < \tau_2$. On the other hand, after the second vaccination, the memory B cells are reactivated by re-exposure to antigen, and this reactivation induces antibody-secreting cells, increases the number of memory B cells, and further re-establishes B cell memory. The recall B cell responses and their antibody secretion are described by the function of $P_2(M_1(t) + M_2(t))^m/((M_1(t) + M_2(t))^m + K^m)$ for $\tau_2 + \eta_2 \leq t$. The quantity and quality of memory B cells established by the second vaccination are considered in P_2. In a similar manner, the recall B cell responses by the vaccine booster (i.e., the third dose) are simply described by $P_3(M_1(t) + M_2(t) + M_3(t))^m/((M_1(t) + M_2(t) + M_3(t))^m +$

K^m) for $\tau_3 + \eta_3 \leq t$. Note that $P_2 = P_3$, $\eta_2 = \eta_3$ are assumed in our booster simulations. The other parameters, p and c, represent the antibody production rate and the clearance rate of antibodies, respectively.

Since the clearance rate of antibody is much larger than the decay of antibody-secreting cells, we made a quasi-steady state assumption, $dA(t)/dt = 0$, and replaced Eq.(3) with $A(t) = pB(t)/c$. Thus, we obtained the following simplified mathematical model, which we used to analyze the antibody responses in this study (see **Extended Data Fig 5A**):

$$\frac{dM_i(t)}{dt} = \begin{cases} 0 & (t < \tau_i) \\ -dM_i(t) & (t \geq \tau_i) \end{cases}, \qquad (4)$$

$$\frac{dA(t)}{dt} = H_i(t)\frac{M(t)^m}{K^m + M(t)^m} - \mu A(t), \qquad (5)$$

where $H_i(t) = H_i = pP_i/c$ for $\tau_i + \eta_i \leq t < \tau_{i+1} + \eta_{i+1}$. In our analysis, the variable $A(t)$ corresponds to the IgG(S) titers (AU/mL).

Quantifying vaccine-elicited time-course antibody dynamics

In addition to the participants in the cohort, we included 12 health care workers whose serum was sequentially sampled for 40 days (on average 25 samples per individual) for validation and parameterization of a mathematical model for vaccine-elicited antibody dynamics. A nonlinear mixed effects model was used to fit the antibody dynamics model, given by Eqs.(4-5), to the longitudinal antibody titers of IgG(S) obtained from the 12 health care workers. The mathematical model included both a fixed effect and a random effect in each parameter. That is, the parameters for individual k, $\theta_k (= \theta \times e^{\pi_k})$, are represented as a product of θ (a fixed effect) and e^{π_k} (a random effect). π_k follows a normal distribution with mean 0 and standard deviation Ω. We here assumed that the parameters H_1, H_2, η_1, η_2, and m varied across individuals, whereas we did not consider interindividual variability in other parameters to ensure parameter identifiability. Note that the half-life of mRNA (i.e., $\log 2/d$) and dose of mRNA (i.e., D_i) are assumed to be 1 day[45] and 100 $(\mu g/0.5\mathrm{mL})$[46], respectively. Fixed effect and random effect were

estimated by using the stochastic approximation expectation-approximation algorithm and empirical Bayes' method, respectively. Fitting was performed using MONOLIX 2019R2 (www.lixoft.com)[47]. The estimated (fixed and individual) parameters are listed in **Supplementary Table 4**. Interestingly, we found that most of the best-fitted estimated parameters in the mathematical model (i.e., D_1, D_2, d, μ, K, η_1, η_2, H_1) were the same or similar across the 12 individuals compared with those of parameters of m and H_2 (see **Supplementary Table 4**). We note that m and H_2, which showed wide variation of estimated values, contributed mainly to the vaccine-elicited antibody dynamics after the second vaccination, whereas the other parameters contributed to that after the first dose.

Since 2,407 participants had only 2 or 3 measurements of antibody titers at different time points, we hereafter fixed the parameters in our mathematical model to be the estimated population parameters listed in **Supplementary Table 4**, except m and H_2, to accurately reconstruct the large variations in antibody dynamics after the second dose, and these two parameters were independently estimated from each IgG(S) by a nonlinear least-squares method. Although the variation in the 12 individuals may not cover the whole variation of the antibody induction dynamics after the first dose, our analysis focused on those after peak, and the results on the stratification (in particular, the durable and vulnerable populations) are expected to be the same. Using the estimated parameters for each individual, we fully reconstructed the dynamics of IgG(S) titers after the first vaccination (**Extended Data Fig 5B**). We summarized the distribution of parameter values m and H_2 for 2,407 participants in **Extended Data Fig 5C**, and the best-fit antibody titer curves of 600 randomly selected individuals are plotted along with the observed data for visualization in **Supplementary Fig 2**.

Unsupervised clustering and stratification of antibody dynamics

Unsupervised random forest clustering was performed on the selected features of the vaccine-elicited time-course antibody dynamics (rfUtilities package in R). After a random forest dissimilarity (i.e., the distance matrix between all pairs of samples) was obtained, it was visualized

with Uniform Manifold Approximation and Projection (UMAP) in a two-dimensional plane and was stratified with spectral clustering (Python scikit-learn). The optimal number of clusters was determined by the eigengap heuristic method.

Random forest classifiers for characterizing stratified groups

Random forest classifiers were trained to predict either of the six stratified groups (G1-G6) or their combination (G1/G2, G5/G6) using randomForest and rfPermute packages in R. The receiver operating characteristic (ROC) curve for each classifier was drawn from out-of-bag (OOB) samples using the pROC package in R. Feature importance was based on MeanDecreaseAccuracy and was shown as Chord diagrams (circlize package in R). Only the features with $p < 0.05$ (obtained with 1,000 permutations) were selected.

Statistical analysis

The paper-based questionnaires collected from 2,159 participants were converted into a set of categorical and numerical variables. Numerical variables included age and the interval between the two doses. These variables were then used as input features to random forest classifiers to predict each stratified group (G1-G6). Missing values of categorical variables were treated as a separate category and included in the analyses. The variables used here belonged to any of the following five categories: (i) basic demographic information and lifestyle habits, (ii) information on vaccinations, (iii) underlying medical conditions, (iv) adverse reactions, and (v) medications being taken. As a subanalysis, we also divided participants into three generations according to age (0-39 [young], 40-64 [middle-aged], and 65-100 [old]) and trained random forest classifiers in each generation. When necessary, the same variables were compared among different generations or different groups using Pearson's chi-square test (for categorical variables), analysis of variance (ANOVA, for more than two numerical variables), or Welch T-test (for two numerical variables). The Pearson correlation coefficient was calculated to evaluate the association between a pair of continuous variables. To calculate the correlation matrix between

533 features, we augmented the variables by adding the following three categories to the above five
534 categories: (vi) antibody titers of each individual, (vii) dynamic parameters of each individual, and
535 (viii) dummy variables specifying each stratified group (G1 to G6). The correlation matrix of these
536 variables (features) was used as an input to principal component analysis. All statistical analyses
537 were performed using R (version 4.1.2).

LIST OF SUPPLEMENTARY MATERIALS

REFERENCES

1 Lumley, S. F. *et al.* Antibody Status and Incidence of SARS-CoV-2 Infection in Health Care Workers. *N Engl J Med* **384**, 533-540, doi:10.1056/NEJMoa2034545 (2021).

2 Cromer, D. *et al.* Neutralising antibody titres as predictors of protection against SARS-CoV-2 variants and the impact of boosting: a meta-analysis. *Lancet Microbe* **3**, e52-e61, doi:10.1016/S2666-5247(21)00267-6 (2022).

3 Khoury, D. S. *et al.* Neutralizing antibody levels are highly predictive of immune protection from symptomatic SARS-CoV-2 infection. *Nat Med* **27**, 1205-1211, doi:10.1038/s41591-021-01377-8 (2021).

4 Pegu, A. *et al.* Durability of mRNA-1273 vaccine-induced antibodies against SARS-CoV-2 variants. *Science* **373**, 1372-1377, doi:10.1126/science.abj4176 (2021).

5 Gaebler, C. *et al.* Evolution of antibody immunity to SARS-CoV-2. *Nature* **591**, 639-644, doi:10.1038/s41586-021-03207-w (2021).

6 Goldberg, Y. *et al.* Waning Immunity after the BNT162b2 Vaccine in Israel. *N Engl J Med* **385**, e85, doi:10.1056/NEJMoa2114228 (2021).

7 Khoury, J. *et al.* COVID-19 vaccine - Long term immune decline and breakthrough infections. *Vaccine* **39**, 6984-6989, doi:10.1016/j.vaccine.2021.10.038 (2021).

8 Levin, E. G. *et al.* Waning Immune Humoral Response to BNT162b2 Covid-19 Vaccine over 6 Months. *N Engl J Med* **385**, e84, doi:10.1056/NEJMoa2114583 (2021).

9 Wheatley, A. K. *et al.* Evolution of immune responses to SARS-CoV-2 in mild-moderate COVID-19. *Nat Commun* **12**, 1162, doi:10.1038/s41467-021-21444-5 (2021).

10 Cele, S. *et al.* Omicron extensively but incompletely escapes Pfizer BNT162b2 neutralization. *Nature* **602**, 654-656, doi:10.1038/s41586-021-04387-1 (2022).

11 Keehner, J. *et al.* Resurgence of SARS-CoV-2 Infection in a Highly Vaccinated Health System Workforce. *N Engl J Med* **385**, 1330-1332, doi:10.1056/NEJMc2112981 (2021).

12 Kotaki, R. *et al.* SARS-CoV-2 Omicron-neutralizing memory B-cells are elicited by two doses of BNT162b2 mRNA vaccine. *Sci Immunol*, eabn8590, doi:10.1126/sciimmunol.abn8590 (2022).

13 Perez-Then, E. *et al.* Neutralizing antibodies against the SARS-CoV-2 Delta and Omicron variants following heterologous CoronaVac plus BNT162b2 booster vaccination. *Nat Med* **28**, 481-485, doi:10.1038/s41591-022-01705-6 (2022).

14 Falsey, A. R. *et al.* SARS-CoV-2 Neutralization with BNT162b2 Vaccine Dose 3. *N Engl J Med* **385**, 1627-1629, doi:10.1056/NEJMc2113468 (2021).

15 Goel, R. R. *et al.* Efficient recall of Omicron-reactive B cell memory after a third dose of SARS-CoV-2 mRNA vaccine. *bioRxiv*, doi:10.1101/2022.02.20.481163 (2022).

16 Muik, A. *et al.* Neutralization of SARS-CoV-2 Omicron by BNT162b2 mRNA vaccine-elicited human sera. *Science* **375**, 678-680, doi:10.1126/science.abn7591 (2022).

17 Xia, H. *et al.* Neutralization and durability of 2 or 3 doses of the BNT162b2 vaccine against Omicron SARS-CoV-2. *Cell Host Microbe*, doi:10.1016/j.chom.2022.02.015 (2022).

18 Choi, A. *et al.* Safety and immunogenicity of SARS-CoV-2 variant mRNA vaccine boosters in healthy adults: an interim analysis. *Nat Med* **27**, 2025-2031, doi:10.1038/s41591-021-01527-y (2021).

19 Juno, J. A. & Wheatley, A. K. Boosting immunity to COVID-19 vaccines. *Nat Med* **27**, 1874-1875, doi:10.1038/s41591-021-01560-x (2021).

20 Shroff, R. T. *et al.* Immune responses to two and three doses of the BNT162b2 mRNA vaccine in adults with solid tumors. *Nat Med* **27**, 2002-2011, doi:10.1038/s41591-021-01542-z (2021).

21 Wei, J. *et al.* Antibody responses to SARS-CoV-2 vaccines in 45,965 adults from the general population of the United Kingdom. *Nat Microbiol* **6**, 1140-1149, doi:10.1038/s41564-021-00947-3 (2021).

22 Lustig, Y. *et al.* BNT162b2 COVID-19 vaccine and correlates of humoral immune responses and dynamics: a prospective, single-centre, longitudinal cohort study in health-care workers. *Lancet Respir Med* **9**, 999-1009, doi:10.1016/S2213-2600(21)00220-4 (2021).

23 Kobashi, Y. *et al.* Seroprevalence of SARS-CoV-2 antibodies among hospital staff in rural Central Fukushima, Japan: A historical cohort study. *Int Immunopharmacol* **98**, 107884, doi:10.1016/j.intimp.2021.107884 (2021).

24 Kobashi, Y. *et al.* The difference between IgM and IgG antibody prevalence in different serological assays for COVID-19; lessons from the examination of healthcare workers. *Int Immunopharmacol* **92**, 107360, doi:10.1016/j.intimp.2020.107360 (2021).

25 Nakano, Y. *et al.* Time course of the sensitivity and specificity of anti-SARS-CoV-2 IgM and IgG antibodies for symptomatic COVID-19 in Japan. *Sci Rep* **11**, 2776, doi:10.1038/s41598-021-82428-5 (2021).

26 *Quantitative IgG antibodies to Spike protein of SARS-CoV-2*, <https://icahn.mssm.edu/files/ISMMS/Assets/Departments/Pathology/COVQI_Link-to-Test-Information-and-Interpretation.pdf> (2020).

27 Lucas, C. *et al.* Impact of circulating SARS-CoV-2 variants on mRNA vaccine-induced immunity. *Nature* **600**, 523-529, doi:10.1038/s41586-021-04085-y (2021).

28 *Population Estimates by Age (Five-Year Groups) and Sex - July 1, 2021*, <https://www.stat.go.jp/data/jinsui/pdf/202112.pdf> (2021).

29 Ward, H. *et al.* Population antibody responses following COVID-19 vaccination in 212,102 individuals. *Nat Commun* **13**, 907, doi:10.1038/s41467-022-28527-x (2022).

30 Yau, K. *et al.* Evaluation of the SARS-CoV-2 Antibody Response to the BNT162b2 Vaccine in Patients Undergoing Hemodialysis. *JAMA Netw Open* **4**, e2123622, doi:10.1001/jamanetworkopen.2021.23622 (2021).

31 Moyon, Q. *et al.* BNT162b2 vaccine-induced humoral and cellular responses against SARS-CoV-2 variants in systemic lupus erythematosus. *Ann Rheum Dis* **81**, 575-583, doi:10.1136/annrheumdis-2021-221097 (2022).

32 Shroff, R. T. *et al.* Immune responses to two and three doses of the BNT162b2 mRNA vaccine in adults with solid tumors. *Nat Med* **27**, 2002-2011, doi:10.1038/s41591-021-01542-z (2021).

33 Goel, R. R. *et al.* mRNA vaccines induce durable immune memory to SARS-CoV-2 and variants of concern. *Science* **374**, abm0829, doi:10.1126/science.abm0829 (2021).

34 Feng, S. *et al.* Correlates of protection against symptomatic and asymptomatic SARS-CoV-2 infection. *Nat Med* **27**, 2032-2040, doi:10.1038/s41591-021-01540-1 (2021).

35 Costiniuk, C. T. *et al.* CTN 328: immunogenicity outcomes in people living with HIV in Canada following vaccination for COVID-19 (HIV-COV): protocol for an observational cohort study. *BMJ Open* **11**, e054208, doi:10.1136/bmjopen-2021-054208 (2021).

36 Di Noia, V. *et al.* Rapid decline of humoral response to two doses of BNT162b2 vaccine in patients with solid cancer after six months: The urgent need of the additional dose! *Eur J Cancer* **165**, 169-173, doi:10.1016/j.ejca.2022.01.011 (2022).

37 Fenioux, C. *et al.* SARS-CoV-2 Antibody Response to 2 or 3 Doses of the BNT162b2 Vaccine in Patients Treated With Anticancer Agents. *JAMA Oncol*, doi:10.1001/jamaoncol.2021.7777 (2022).

38 Ramasamy, M. N. *et al.* Safety and immunogenicity of ChAdOx1 nCoV-19 vaccine administered in a prime-boost regimen in young and old adults (COV002): a single-blind, randomised, controlled, phase 2/3 trial. *Lancet* **396**, 1979-1993, doi:10.1016/s0140-6736(20)32466-1 (2021).

39 Juno, J. A. *et al.* Humoral and circulating follicular helper T cell responses in recovered patients with COVID-19. *Nat Med* **26**, 1428-1434, doi:10.1038/s41591-020-0995-0 (2020).

40 Turner, J. S. *et al.* SARS-CoV-2 mRNA vaccines induce persistent human germinal centre responses. *Nature* **596**, 109-113, doi:10.1038/s41586-021-03738-2 (2021).

41 Turner, J. S. *et al.* SARS-CoV-2 infection induces long-lived bone marrow plasma cells in humans. *Nature* **595**, 421-425, doi:10.1038/s41586-021-03647-4 (2021).

42 Kim, W. *et al.* Germinal centre-driven maturation of B cell response to mRNA vaccination. *Nature* **604**, 141-145, doi:10.1038/s41586-022-04527-1 (2022).

43 Burki, T. K. Fourth dose of COVID-19 vaccines in Israel. *Lancet Respir Med* **10**, e19, doi:10.1016/S2213-2600(22)00010-8 (2022).

44 Abbasi, J. Fourth COVID-19 Vaccine Dose Increases Low Antibodies. *JAMA* **327**, 517, doi:10.1001/jama.2022.0727 (2022).

45 Anand, P. & Stahel, V. P. Correction to: The safety of Covid-19 mRNA vaccines: a review. *Patient Saf Surg* **15**, 22, doi:10.1186/s13037-021-00296-4 (2021).

46 Lin, D. Y. *et al.* Effectiveness of Covid-19 Vaccines over a 9-Month Period in North Carolina. *N Engl J Med* **386**, 933-941, doi:10.1056/NEJMoa2117128 (2022).

47 Traynard, P., Ayral, G., Twarogowska, M. & Chauvin, J. Efficient Pharmacokinetic Modeling Workflow With the MonolixSuite: A Case Study of Remifentanil. *CPT Pharmacometrics Syst Pharmacol* **9**, 198-210, doi:10.1002/psp4.12500 (2020).

48 *April 2021 Survey Population and Households by Municipality (Japanese Residents + Foreign Residents) (Japanese)*, <https://www.kokudo.or.jp/service/data/map/fukushima.pdf> (2021).

49 *The incidence of COVID-19 in Fukushima Prefecture (Japanese)*, <https://www.pref.fukushima.lg.jp/sec/21045c/fukushima-hasseijyoukyou.html> (2021).

ACKNOWLEDGMENTS

We would like to thank all the staff from Fukushima Medical University, Seireikai health care group, Hirata village office, Soma City office, Soma Central Hospital, Soma General Hospital, Minamisoma City office, Minamisoma City Medical Association, Minamisoma Municipal General Hospital, Shindo Clinic and Medical Governance Institute, who contributed significantly to the accomplishment of this research, especially, Ms. Yuka Harada, Ms. Serina Noji, Ms. Naomi Ito, Dr. Makoto Kosaka, Mr. Anju Murayama, Mr. Sota Sugiura, Mr. Manato Tanaka, Ms. Yuna Uchi, Mr. Yudai Kaneda, Mr. Masahiko Nihei, Mr. Hideo Sato, Ms. Rie Yanai, Ms. Yasuko Suzuki, Ms. Keiko Abe, Dr. Hidekiyo Tachiya, Mr. Kouki Nakatsuka, Dr. Ryuzaburo Shineha, Ms. Miki Sato, Dr. Masahiko Sato, Mr. Naoharu Tadano, Mr. Kazuo Momma, Mr. Shu-ichi Mori, Ms. Saori Yoshisato, Ms. Katsuko Onoda, Mr. Satoshi Kowata, Mr. Masatsugu Tanaki, Dr. Tomoyoshi Oikawa, Dr. Joji Shindo, Ms. Xujin Zhu, Ms. Asaka Saito, Ms. Yuumi Kondo, and Ms. Tomoyo Nishimura. This study was supported by Medical & Biological Laboratories Co., Ltd., Shenzhen YHLO Biotech Co., Ltd., the distributor and manufacturer of the antibody measurement system (iFlash 3000), Research Center for Advanced Science and Technology in the University of Tokyo, and in part by a National Research Foundation of Korea (NRF) grant funded by the Korea government (MSIT) (2022R1C1C2003637) (to K.S.K.); a Grant-in-Aid for JSPS Scientific Research (KAKENHI) B 18H01139 (to S.I.), 16H04845 (to S.I.), Scientific Research in Innovative Areas 20H05042 (to S.I.); AMED CREST 19gm1310002 (to S.I.); AMED Development of Vaccines for the Novel Coronavirus Disease, 21nf0101638s0201 (to S.I.), 21nf0101638h0001 (to M.T.); AMED Japan Program for Infectious Diseases Research and Infrastructure, 20wm0325007h0001 (to S.I.), 20wm0325004s0201 (to S.I.), 20wm0325012s0301 (to S.I.), 20wm0325015s0301 (to S.I.); AMED Research Program on HIV/AIDS 22fk0410052s0401 (to S.I.); AMED Research Program on Emerging and Re-emerging Infectious Diseases 20fk0108140s0801 (to S.I.); AMED Program for Basic and Clinical Research on Hepatitis 21fk0210094 (to S.I.); AMED Program on the Innovative Development and the Application of New Drugs for Hepatitis B 22fk0310504h0501 (to S.I.); AMED Strategic Research Program for Brain

Sciences 22wm0425011s0302; AMED JP22dm0307009 (to K.A.); JST MIRAI JPMJMI22G1 (to S.I.); Moonshot R&D JPMJMS2021 (to K.A. and S.I.) and JPMJMS2025 (to S.I.); Institute of AI and Beyond at the University of Tokyo (to K.A.); Mitsui Life Social Welfare Foundation (to S.I.); Shin-Nihon of Advanced Medical Research (to S.I.); Suzuken Memorial Foundation (to S.I.); Life Science Foundation of Japan (to S.I.); SECOM Science and Technology Foundation (to S.I.); The Japan Prize Foundation (to S.I.); Foundation of Kinoshita Memorial Enterprise (to S.I.); and Kowa Co (to M.T.).

AUTHOR CONTRIBUTIONS

SI and MT designed the research. YKobashi, YS, TZ, YN, FO, MTa, CY, KS, and MTs conducted the data collection and curation. YT, MK, MY, TA, YS, SN, TK, AS, AN, YS and YKaneko carried out the investigations. NN, KSK, DT, MA, SIwanami, KA, and SI carried out the computational analysis. SI and MT supervised the project. All authors contributed to writing the manuscript.

COMPETING FINANCIAL INTERESTS

YKaneko is employed by Medical & Biological Laboratories, Co. (MBL, Tokyo, Japan). MBL imported the testing material used in this research. YKaneko participated in the testing process; however, he did not engage in the research design and analysis. YKobashi and MT received a research grant from Pfizer Health Research Foundation for research not associated with this work.

INSTITUTIONAL REVIEW BOARD STATEMENT

This study was approved by the ethics committees of Hirata Central Hospital (number 2021-0611-1) and Fukushima Medical University (number 2021-116). This study was conducted in accordance with the Code of Ethics of the World Medical Association (Declaration of Helsinki).

INFORMED CONSENT STATEMENT

Informed consent was obtained from all subjects involved in the study.

EXTENDED DATA FIGURES

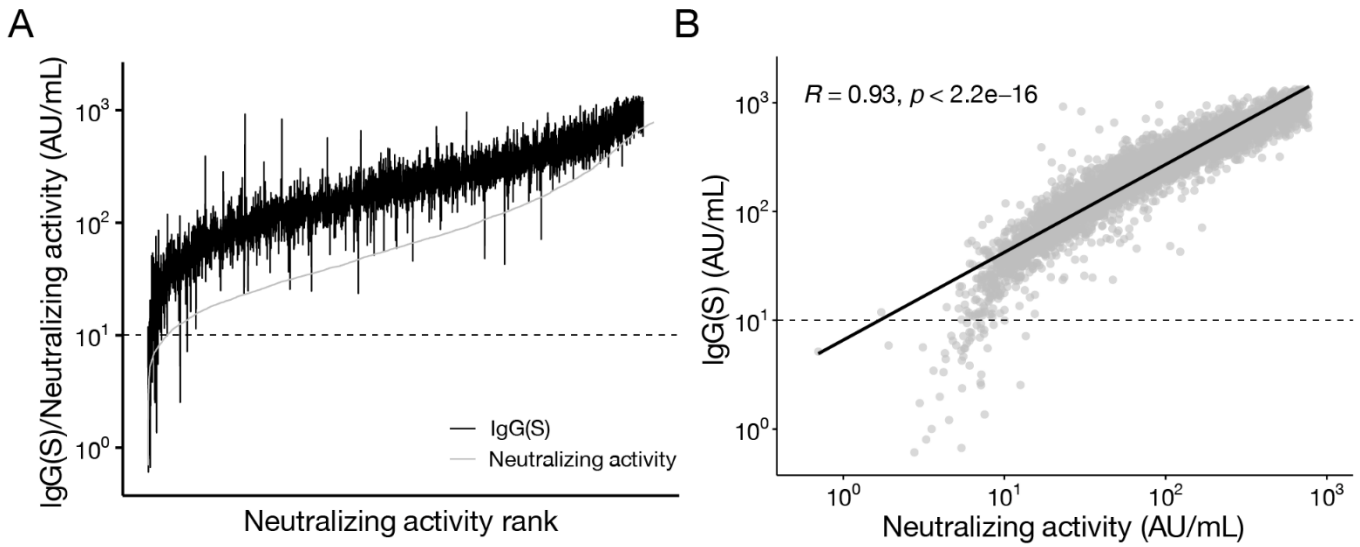

Extended Data Figure 1 | Comparison between IgG(S) and neutralization activity: (A) Curve with IgG(S) and neutralization activity on the *Y*-axis and its corresponding neutralization activity rank on the *X*-axis are plotted in black and gray, respectively. **(B)** Correlations between IgG(S) and neutralization activity from same samples are described. Data points represent individual samples. Correlations were calculated as Pearson correlation coefficients.

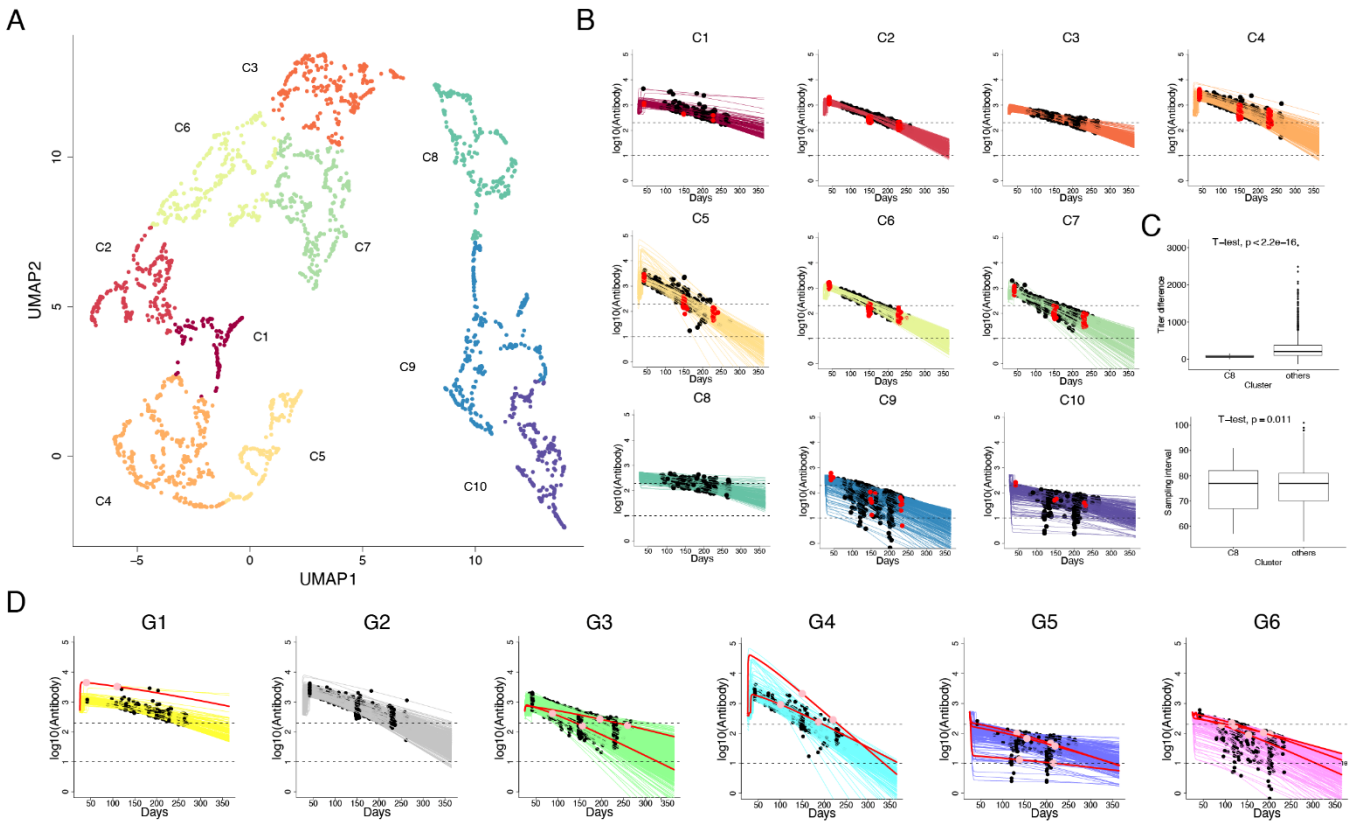

Extended Data Figure 2 | Clustering vaccine-elicited antibody response: (A) UMAP of 10 clustered antibody responses based on the extracted features from the reconstructed individual-level antibody dynamics are shown. Data points represent individual participants and are colored by the 10 clusters (i.e., C1 to C10). **(B)** Reconstructed individual antibody dynamics after 25 days after the first vaccination in each cluster in the different colors are represented along with the measured IgG(S). The black and red circles correspond to individuals who had 2 or 3 measurements of antibody titers at different time points, respectively. **(C)** The difference in antibody titers between the two measurements and its sampling interval are compared among clusters. **(D)** Reconstructed individual antibody dynamics after 25 days after the first vaccination in each group in the different colors are represented along with the measured IgG(S) in black and red corresponding to individuals who had 2 or 3 measurements, respectively. The red curves indicate individuals who were infected with SARS-CoV-2 or whose family was infected. The horizontal dashed lines correspond to 200 and 10 AU/mL, respectively.

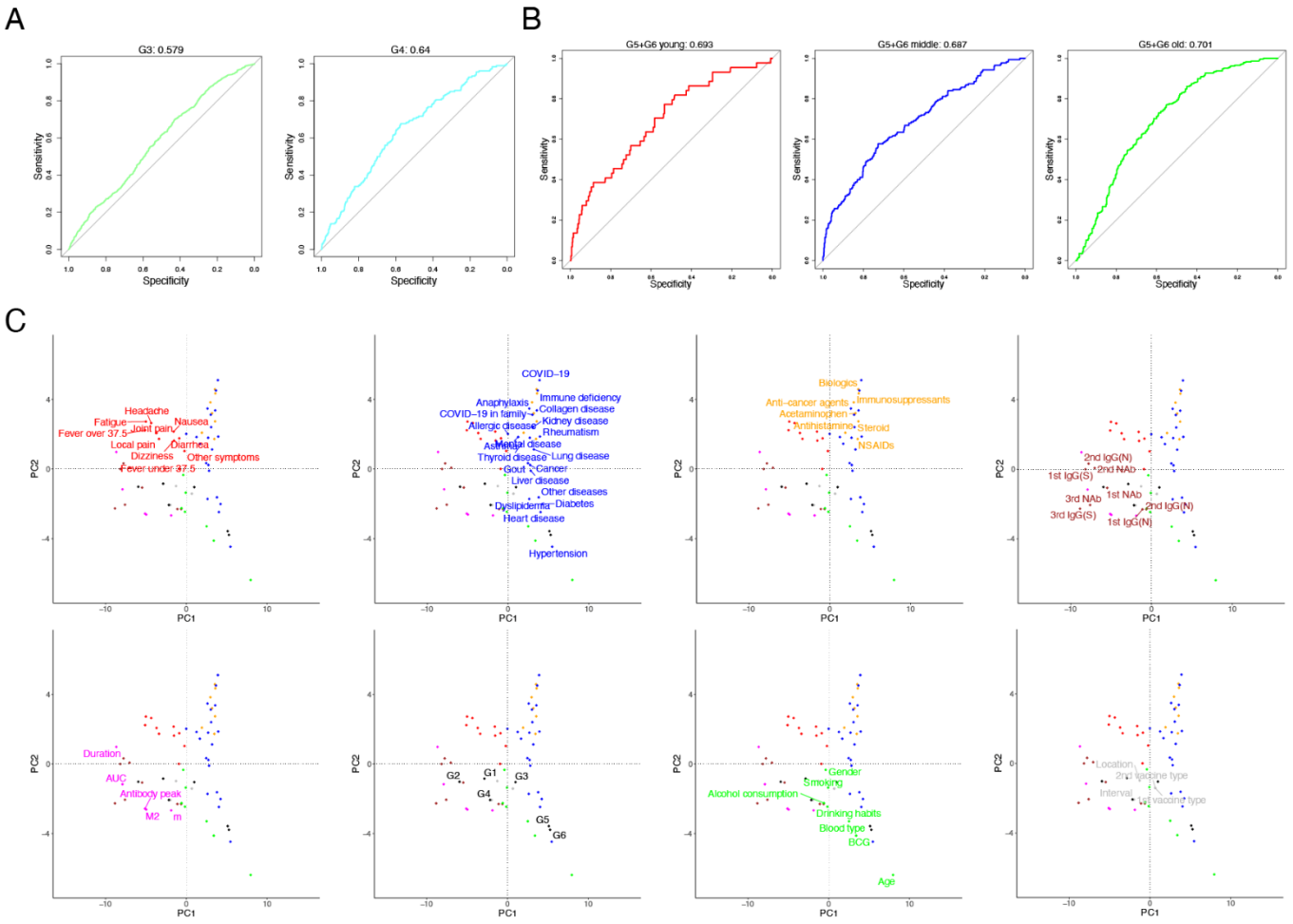

744 **Extended Data Figure 3 | Characterization of stratification: (A)** and **(B)** The ROC curves of
745 random forest classifiers trained on predicting G3, G4, or G5/G6 in young, middle-aged, and old
746 populations are shown, respectively. The corresponding AUC value of each ROC curve is
747 calculated on the top of each panel. **(C)** Name labels of **Figure 3D** (principal component analysis
748 of features) are shown.

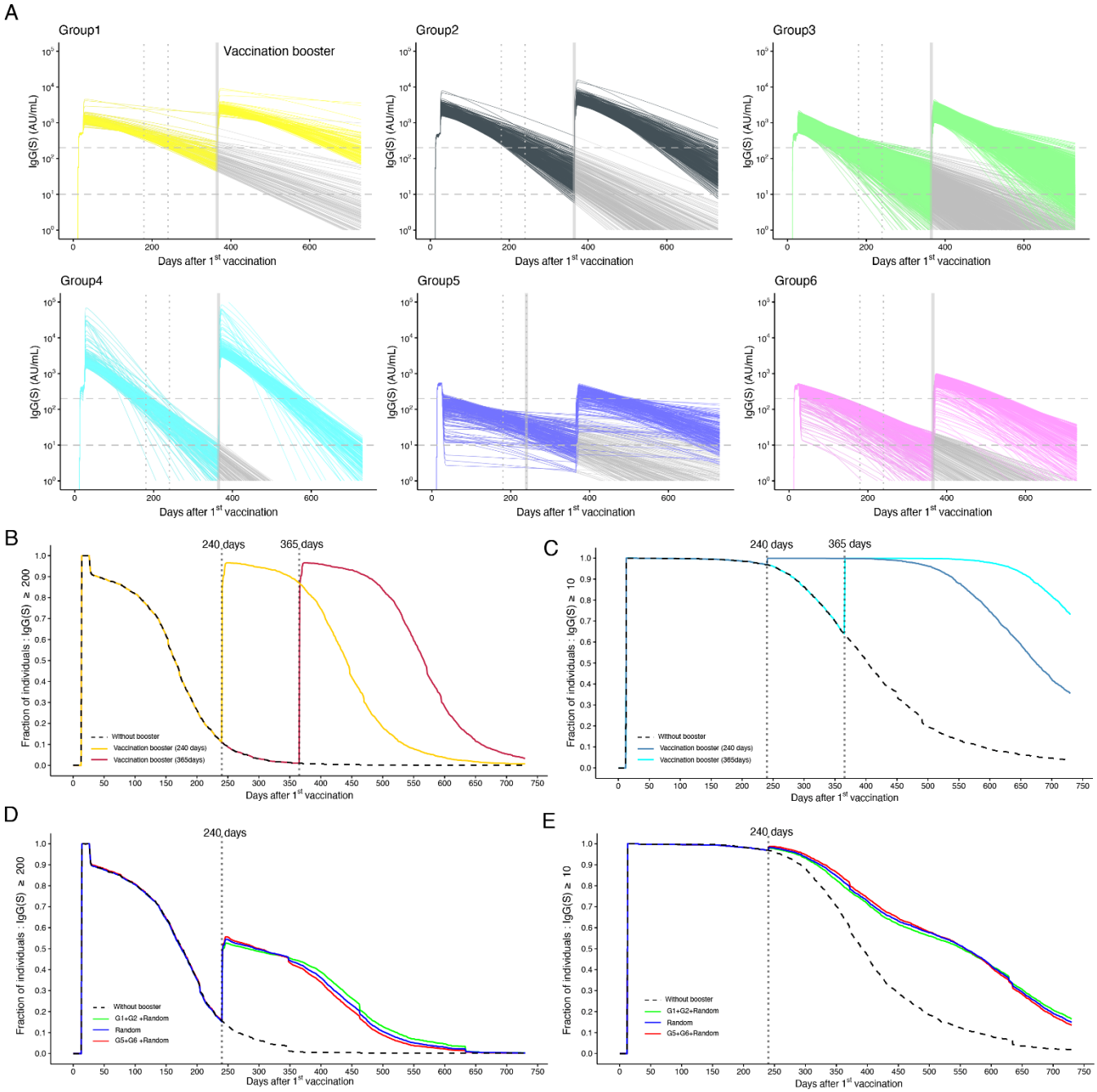

749 **Extended Data Figure 4 | Simulating booster vaccines under different scenarios: (A)**
750 Predicted individual elicited antibody responses in each group over the first year after the booster
751 vaccination at 1 year after the first vaccination are shown. The horizontal dashed and vertical
752 dotted lines correspond to 200 and 10 AU/mL and at 180 and 240 days after the first vaccination,
753 respectively. **(B)** and **(C)** show the fractions of individuals with antibody titers above 200 and 10
754 AU/mL with (i.e., colored curves) and without (i.e., black dashed curve) 100% booster vaccination
755 at 240 and 365 days after the first vaccination, respectively. **(D)** and **(E)** show those above 200
756 and 10 AU/mL with and without 50% booster vaccination at 240 days after the first vaccination,
757 respectively. The green, blue, and red curves correspond to the booster vaccination targeting
758 individuals randomly sampled from “in addition G1/G2, extra are from G1-G6”, “G1-G6”, and “in
759 addition G5/G6, extra are from G1-G6”, respectively.

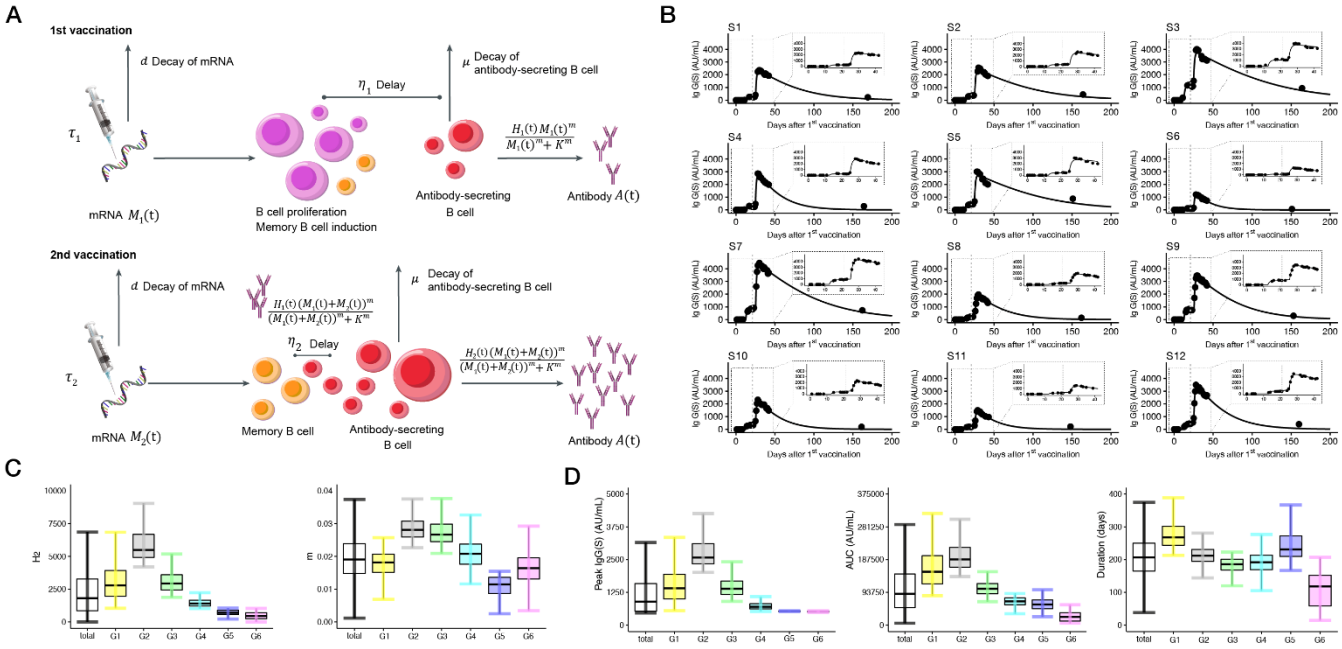

760 **Extended Data Figure 5 | Quantification of vaccine-elicited antibody dynamics: (A)**
761 Schematic diagram of mathematical modeling. **(B)** Observed and fitted IgG(S) titers for individual
762 participants are described. The IgG(S) titers are obtained from the 12 health care workers with
763 sequentially sampled serum for 40 days (on average 25 samples per individual). Enlarged view
764 of the dotted box shows a fine-level plot focusing on the early period. The dashed vertical lines at
765 day 21 correspond to the date of second vaccination. **(C)** Distributions of estimated parameter
766 values of H_2 and m for 2,407 participants are plotted, respectively, among total or stratified
767 populations. **(D)** Distributions of the extracted features from the reconstructed individual-level
768 antibody dynamics are plotted, respectively, among total or stratified populations.

769 **Extended Data Table 1 | Basic demographics for the Fukushima vaccination cohort**

Characteristic	<40 years	40-64 years	>65 years	Overall	p-value
Gender					0.001
Male	338(46.8)	421(38.2)	286(40.8)	1045(41.4)	
Vaccine type					0.015
BNT162b2(Pfizer–BioNTech)	651(90.0)	971(88.1)	649(92.6)	2271(89.9)	
mRNA-1273(Moderna)	0(0.0)	3(0.3)	0(0.0)	3(0.1)	
Days (mean [SD])					
from 1st dose	106.3[37.7]	104.4[35.1]	103.8[17.2]	104.8[32.0]	0.302
from 2nd dose	181.4[37.5]	180.1[35.7]	180.1[16.9]	180.5[32.2]	0.292
Blood type					
A	239(35.7)	427(39.0)	212(35.4)	878(37.2)	<0.001
B	151(22.6)	236(21.6)	140(23.4)	527(22.3)	<0.001
O	213(31.8)	326(29.8)	172(28.7)	711(30.1)	0.367
AB	66(9.9)	105(9.6)	75(12.5)	246(10.4)	0.432
BCG history	560(83.5)	907(83.1)	412(61.9)	1879(77.4)	0.395
Smoking	144(19.9)	253(23.0)	63(9.0)	460(18.2)	<0.001
Drinking habits					<0.001
Almost not	403(55.7)	542(49.2)	458(65.3)	1403(55.5)	
Occasionally	247(34.2)	310(28.1)	90(12.8)	647(25.6)	
Everyday	63(8.7)	222(20.2)	127(18.1)	412(16.3)	
Daily Alcohol Consumption					<0.001
<20g	322(44.5)	382(34.7)	176(25.1)	880(34.8)	
20-40g	108(14.9)	214(19.4)	87(12.4)	409(16.2)	
40-60g	20(2.8)	60(5.4)	20(2.9)	100(4.0)	
>60g	5(0.7)	13(1.2)	2(0.3)	20(0.8)	
Comorbidities					
Hypertension	8(1.1)	237(21.5)	432(61.6)	677(26.8)	<0.001
Dyslipidemia	12(1.7)	123(11.2)	146(20.8)	281(11.1)	<0.001
Heart disease	14(1.9)	47(4.3)	140(20.0)	201(8.0)	<0.001
Diabetes	6(0.8)	72(6.5)	110(15.7)	188(7.4)	<0.001
Allergic disease	69(9.5)	95(8.6)	21(3.0)	185(7.3)	<0.001
Asthma	49(6.8)	45(4.1)	28(4.0)	122(4.8)	0.079
Liver disease	11(1.5)	45(4.1)	58(8.3)	114(4.5)	<0.001
Cancer	3(0.4)	35(3.2)	46(6.6)	84(3.3)	<0.001
Gout	5(0.7)	45(4.1)	26(3.7)	76(3.0)	0.001
Thyroid disease	8(1.1)	40(3.6)	11(1.6)	59(2.3)	0.005
Lung disease	12(1.7)	11(1.0)	28(4.0)	51(2.0)	<0.001
Mental disease	17(2.4)	16(1.5)	13(1.9)	46(1.8)	0.739
Rheumatism	2(0.3)	16(1.5)	19(2.7)	37(1.5)	0.006
Kidney disease	6(0.8)	7(0.6)	14(2.0)	27(1.1)	0.089
Anaphylaxis	6(0.8)	7(0.6)	5(0.7)	18(0.7)	0.994
Collagen disease	4(0.6)	6(0.5)	5(0.7)	15(0.6)	0.993
COVID-19 (family)	4(0.6)	5(0.5)	1(0.1)	10(0.4)	0.793
COVID-19	0(0.0)	3(0.3)	4(0.6)	7(0.3)	0.38
Immune deficiency	2(0.3)	4(0.4)	0(0.0)	6(0.2)	0.654
Others	51(7.1)	147(13.3)	189(27.0)	387(15.3)	<0.001
Drug					
Steroid	9(1.2)	23(2.1)	26(3.7)	58(2.3)	0.002
NSAIDs	31(4.3)	78(7.1)	82(11.7)	191(7.6)	<0.001
Acetaminophen	8(1.1)	22(2.0)	30(4.3)	60(2.4)	<0.001
Antihistamine	46(6.4)	65(5.9)	43(6.1)	154(6.1)	0.367
Immunosuppressants	6(0.8)	10(0.9)	8(1.1)	24(1.0)	0.432

Biologics	2(0.3)	5(0.5)	4(0.6)	11(0.4)	0.395
Anti-cancer agent	0(0.0)	5(0.5)	5(0.7)	10(0.4)	0.292
Adverse Reaction					
Local pain	515(71.2)	684(62.1)	228(32.5)	1427(56.5)	<0.001
Fatigue	511(70.7)	627(56.9)	119(17.0)	1257(49.8)	<0.001
Joint pain	327(45.2)	354(32.1)	90(2.8)	771(30.5)	<0.001
Fever (over 37.5 degree)	370(51.2)	308(28.0)	41(5.9)	719(28.5)	<0.001
Headache	321(44.4)	331(30.0)	34(4.9)	686(27.2)	<0.001
Fever (under 37.5 degree)	137(19.0)	209(19.0)	40(5.7)	386(15.3)	<0.001
Dizziness	57(7.9)	45(4.1)	9(1.3)	111(4.4)	<0.001
Nausea	51(7.1)	41(3.7)	6(0.9)	98(3.9)	<0.001
Diarrhea	30(4.2)	25(2.3)	3(0.4)	58(2.3)	<0.001
Others	40(5.5)	69(6.3)	16(2.3)	125(5.0)	0.003

Supplementary Information

Stratifying elicited antibody dynamics after two doses of SARS-CoV-2 vaccine in a community-based cohort in Fukushima, Japan

Naotoshi Nakamura[1,†], Yurie Kobashi[2,3,†], Kwang Su Kim[1,4,5,†], Yuta Tani[6], Yuzo Shimazu[2], Tianchen Zhao[2], Yoshitaka Nishikawa[3], Fumiya Omata[3], Moe Kawashima[2], Makoto Yoshida[6], Toshiki Abe[2], Yoshika Saito[6], Yuki Senoo[6], Saori Nonaka[2], Morihito Takita[2], Chika Yamamoto[2], Takeshi Kawamura[7,8], Akira Sugiyama[7], Aya Nakayama[7], Yudai Kaneko[8,9], Hyeongki Park[1], Yong Dam Jeong[1,5], Daiki Tatematsu[1], Marwa Akao[1], Yoshitaka Sato[10], Shoya Iwanami[1], Yasuhisa Fujita[1], Masatoshi Wakui[11], Kazuyuki Aihara[12], Tatsuhiko Kodama[8], Kenji Shibuya[13,14], Shingo Iwami[1,16,17,18,19,20,‡,*] and Masaharu Tsubokura[2,3,6,20,‡,]

[1]interdisciplinary Biology Laboratory (iBLab), Division of Natural Science, Graduate School of Science, Nagoya University, Nagoya, Japan. [2]Department of Radiation Health Management, Fukushima Medical University School of Medicine, Fukushima, Japan. [3]Department of General Internal Medicine, Hirata Central Hospital, Fukushima, Japan. [4]Department of Science System Simulation, Pukyong National University, Busan, South Korea. [5]Department of Mathematics, Pusan National University, Busan, South Korea. [6]Medical Governance Research Institute, Tokyo, Japan. [7]Proteomics Laboratory, Isotope Science Center, The University of Tokyo, Tokyo, Japan. [8]Laboratory for Systems Biology and Medicine, Research Center for Advanced Science and Technology, The University of Tokyo, Tokyo, Japan. [9]Medical & Biological Laboratories Co., Ltd, Tokyo, Japan. [10]Department of Virology, Nagoya University Graduate School of Medicine, Nagoya, Japan. [11]Department of Laboratory Medicine, Keio University School of Medicine, Tokyo, Japan. [12]International Research Center for Neurointelligence, The University of Tokyo Institutes for Advanced Study, The University of Tokyo, Tokyo, Japan. [13]Soma Medical Center of vaccination for COVID-19, Fukushima, Japan. [14]Tokyo Foundation for Policy Research, Tokyo, Japan. [15]Institute of Mathematics for Industry, Kyushu University, Fukuoka, Japan. [16]Institute for the Advanced Study of Human Biology (ASHBi), Kyoto University, Kyoto, Japan. [17]Interdisciplinary Theoretical and Mathematical Sciences Program (iTHEMS), RIKEN, Saitama, Japan. [18]NEXT-Ganken Program, Japanese Foundation for Cancer Research (JFCR), Tokyo, Japan. [19]Science Groove Inc., Fukuoka, Japan. [20]Minamisoma Municipal General Hospital, Fukushima, Japan.

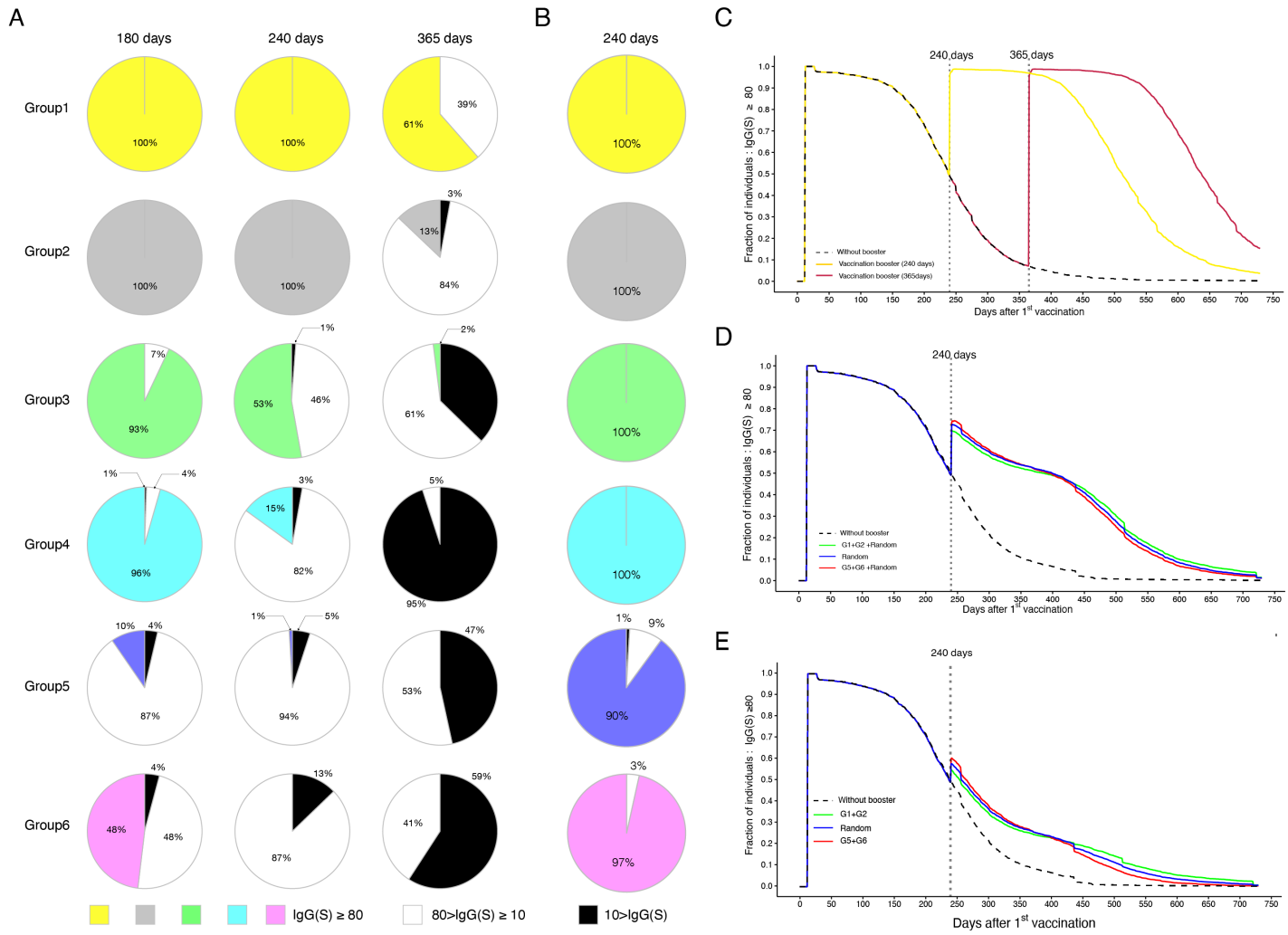

Supplementary Figure 1. Sensitivity analysis on different thresholds of vaccine efficacy: (A) and **(B)** show the fractions of individuals with antibody titers of <10, 10-80, and 80 < AU/mL in each group at 180, 240, and 365 days after the first vaccination and at 1 month post-booster vaccination plotted as black, white, and group color, respectively (for 200 AU/mL, corresponding to **Fig 2H** and **Fig 4B**). **(C)**, **(D)**, and **(E)** represent the time-dependent fractions of individuals with antibody titers above 80 AU/mL with (i.e., colored curves) and without (i.e., black dashed curve) 100%, 50%, and 20% booster vaccination at 240 days (and 365 days for 100% booster vaccination) after the first vaccination, respectively, similar to **Extended Data Fig 4B**, **Fig 4D** and **Extended Data Fig 4D** for 200 AU/mL of the threshold.

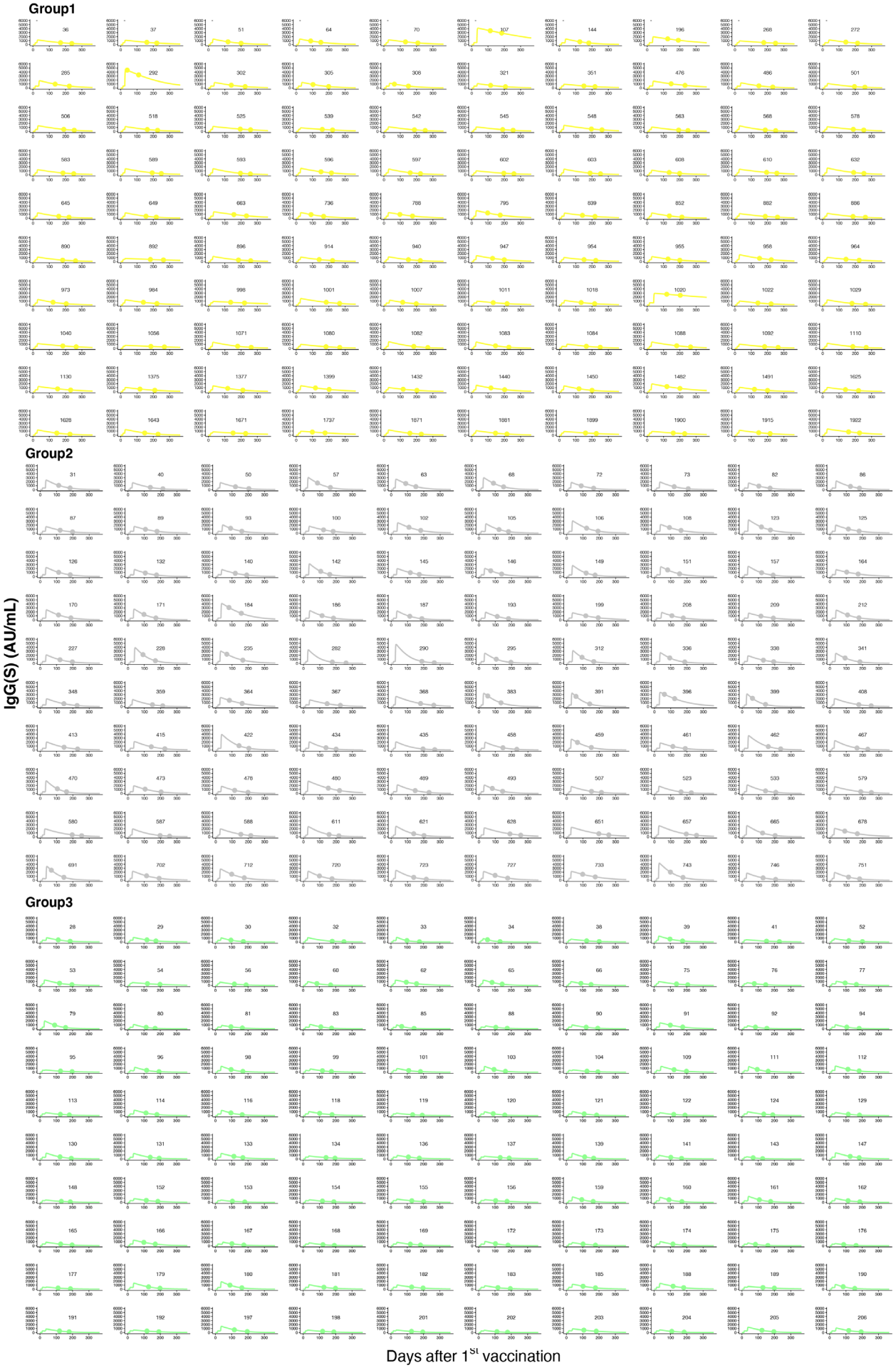
Group1
36
37
51
64
70
107
144
196
268
272
285
292
302
305
306
321
351
476
486
501
506
518
525
539
542
545
548
563
568
578
583
589
593
596
597
602
603
608
610
632
645
649
663
736
788
795
839
852
882
886
890
892
896
914
940
947
954
955
958
964
973
984
998
1001
1007
1011
1018
1020
1022
1029
1040
1056
1071
1080
1082
1083
1084
1088
1092
1110
1130
1375
1377
1399
1432
1440
1450
1482
1491
1625
1628
1643
1671
1737
1871
1881
1899
1900
1915
1922
Group2
31
40
50
57
63
68
72
73
82
86
87
89
93
100
102
105
106
108
123
125
126
132
140
142
145
146
149
151
157
164
170
171
184
186
187
193
199
208
209
212
227
228
235
282
290
295
312
336
338
341
348
359
364
367
368
383
391
396
399
408
413
415
422
434
435
458
459
461
462
467
470
473
478
480
489
493
507
523
533
579
580
587
588
611
621
628
651
657
665
678
691
702
712
720
723
727
733
743
746
751
Group3
28
29
30
32
33
34
38
39
41
52
53
54
56
60
62
65
66
75
76
77
79
80
81
83
85
88
90
91
92
94
95
96
98
99
101
103
104
109
111
112
113
114
116
118
119
120
121
122
124
129
130
131
133
134
136
137
139
141
143
147
148
152
153
154
155
156
159
160
161
162
165
166
167
168
169
172
173
174
175
176
177
179
180
181
182
183
185
188
189
190
191
192
197
198
201
202
203
204
205
206
IgG(S) (AU/mL)
Days after 1st vaccination

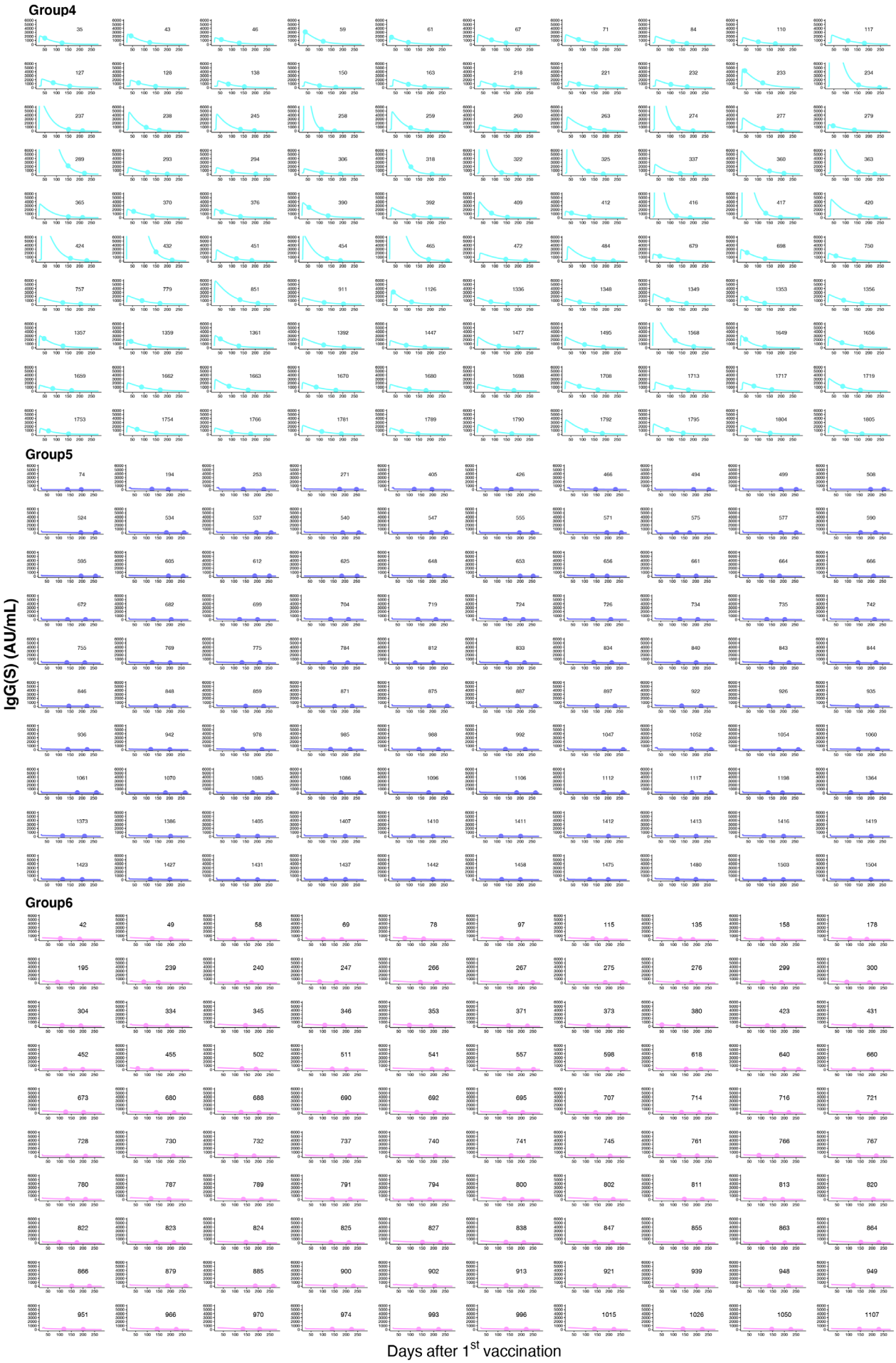
Group4
35 43 46 59 61 67 71 84 110 117
127 128 138 150 163 218 221 232 233 234
237 238 245 258 259 260 263 274 277 279
289 293 294 306 318 322 325 337 360 363
365 370 376 390 392 409 412 416 417 420
424 432 451 454 465 472 484 679 698 750
757 779 851 911 1126 1336 1348 1349 1353 1356
1357 1359 1361 1392 1447 1477 1495 1568 1649 1656
1659 1662 1663 1670 1680 1698 1708 1713 1717 1719
1753 1754 1766 1781 1789 1790 1792 1795 1804 1805
Group5
74 194 253 271 405 426 466 494 499 508
524 534 537 540 547 555 571 575 577 590
595 605 612 625 648 653 656 661 664 666
672 682 699 704 719 724 726 734 735 742
755 769 775 784 812 833 834 840 843 844
846 848 859 871 875 887 897 922 926 935
936 942 978 985 988 992 1047 1052 1054 1060
1061 1070 1085 1086 1096 1106 1112 1117 1198 1364
1373 1386 1405 1407 1410 1411 1412 1413 1416 1419
1423 1427 1431 1437 1442 1458 1475 1480 1503 1504
Group6
42 49 58 69 78 97 115 135 158 178
195 239 240 247 266 267 275 276 299 300
304 334 345 346 353 371 373 380 423 431
452 455 502 511 541 557 598 618 640 660
673 680 688 690 692 695 707 714 716 721
728 730 732 737 740 741 745 761 766 767
780 787 789 791 794 800 802 811 813 820
822 823 824 825 827 838 847 855 863 864
866 879 885 900 902 913 921 939 948 949
951 966 970 974 993 996 1015 1026 1050 1107
IgG(S) (AU/mL)
Days after 1st vaccination

Supplementary Figure 2. Antibody titer trajectory for individual participants stratified into different groups: The estimated antibody titer for each individual participant (solid lines) along with the observed data (closed dots) are depicted using the best-fit parameter estimates. G1, G2, G3, G4, G5, and G6 are shown in yellow, gray, green, light blue, blue, and pink, respectively. In each group, the curve of 100 was randomly selected for visualization because of the large number.

Supplementary Table 1. Details of query words and results of the literature review

#	Query Word	Results
1	“SARS-CoV-2” [tiab] OR “severe coronavirus disease 2019” [tiab] OR “COVID-19” [tiab] OR “severe acute respiratory syndrome coronavirus 2” [tiab] OR “coronavirus disease 2019” [tiab] OR “COVID-19*” [Mesh] OR “SARS-CoV-2*”	235,156
2	“vaccination*” [tiab] OR “vaccine*” [tiab] OR “NVX-CoV2373” [tiab] OR “CVnCoV“ [tiab] OR “Ad26COV2S” [tiab] OR “BNT162 Vaccine*” [Mesh] OR “ChAdOx1 nCoV-19” [Mesh] OR “COVID-19 Vaccines*” [Mesh] OR “mRNA Vaccines” [Mesh] OR “RNA, Viral” [Mesh] OR “Vaccination*” [Mesh] OR “Vaccine Efficacy*” [Mesh] OR “Vaccines*” [Mesh] OR “2019-nCoV Vaccine mRNA-1273*” [Mesh] OR “Ad26COVS1” [Mesh]	500,257
3	“Antibody level*” [tiab] OR “antibody response*” [tiab] OR “Antibody titer*” [tiab] OR “Humoral and Cellular Response*” [tiab] OR “humoral immune response*” [tiab] OR “humoral response*” [tiab] OR “immune response*” [tiab] OR “immunization” [tiab] OR “immunogenicity” [tiab] OR “Antibodies, Viral” [Mesh] OR “Antibody Formation” [Mesh] OR “Immunity, Humoral*” [Mesh] OR “Immunogenicity, Vaccine*” [Mesh]	557,862
4	“Second dose” [tiab] OR “second SARS-CoV-2 vaccine” [tiab] OR “2nd dose” [tiab] OR “second vaccination” [tiab] OR “two doses” [tiab] OR “two sequential doses” [tiab] OR “Two Vaccine Doses” [tiab] OR “two-dose” [tiab] OR “booster doses” [tiab] OR “second vaccine” [tiab] OR “Immunization, Secondary*” [Mesh]	30,432
5	“Cohort” [tiab] OR “Cross-Sectional” [tiab] OR “Follow-Up Studies” [tiab] OR ”Prospective Studies” [tiab] OR ”Cohort Studies” [Mesh] OR ”Cross-Sectional Studies” [Mesh] OR “Follow-Up Studies” [Mesh] OR “Prospective Studies” [Mesh] OR “Observational Study*” [tiab]	3,119,085
6	1 AND 2	32,087
7	1 AND 2 AND 3	7,561
8	1 AND 2 AND 3 AND 4	1,311
9	1 AND 2 AND 3 AND 4 AND 5	440

Supplementary Table 2. Characteristics of the previously reported cohorts

#	Cohort Size	Study Period	Country	Vaccine Type	Population Characteristics	Interview Sheet	Times of Sampling	Sample 1	Sample 2	Sample final	Number of Participants Included in All Sampling	Samples of Neutralizing Antibody	Sample1 of Neutralizing Antibody	Reference
0	2526	270	Japan	BNT162b2 (Pfizer–BioNTech) or mRNA-1273 (Moderna)	Community	Including	2	2526	2443	2443	2443	Including	2526	This study
1	3,991	200	Israel	BNT162b2 (Pfizer–BioNTech)	HCWs	Including	7	3991	2690	1370	693	Including	681	1
2	2,591	180	Italy	BNT162b2 (Pfizer–BioNTech)	Community	Not Including	4	1725	1641	2591	1215	Not Including	NA	2
3	1,935	90	Italy	BNT162b2 (Pfizer–BioNTech)	HCWs	Not Including	3	1935	NA	NA	NA	Including	1935	3
4	1,506	90	Israel	BNT162b2 (Pfizer–BioNTech)	HCWs	Including	2	1506	1209	1209	1194	Not Including	NA	4
5	1,487	41	Israel	BNT162b2 (Pfizer–BioNTech)	HCWs	Including	5	334	375	1487	22	Including	46	5
6	1,012	102	Turkey	CoronaVac (Sinovac)	HCWs	Including	2	1012	836	836	836	Not Including	NA	6

Supplementary Table 3. Characteristics of the vulnerable population

#	Cohort Size	Vaccine Type	Country	Population Characteristics	Age	Sex	Obesity BMI>30	Immunosuppression	Steroid	Hypertension	Autoimmune disease	Heart disease	Lung disease	Kidney disease	Interval / Joint pain	Fever over 37.5	Other factors（P<0.05）	others factors（P>0.05）	Reference
1	3991	BNT162b2(Pfizer–BioNTech)	Israel	HCWs	+	+	+	+	NA	NA	+	NA	NA	NA	NA	NA	● the presence of two or more coexisting conditions (i.e., hypertension, diabetes, dyslipidemia, or heart, lung, kidney, or liver disease) ● age-sex interaction	NA	1
2	1506	BNT162b2(Pfizer–BioNTech)	Israel	HCWs	+	+	NA	+	−	NA	NA	NA	NA	NA	NA	NA	● Underlying conditions (i.e., hypothyroidism, autoimmune disease, cardiac disease, lung disease, immunodeficiency, chronic renal disease, and active oncological disease)	● age-sex interaction ● Allergic reactions	4
3	1487	BNT162b2(Pfizer–BioNTech)	Israel	HCWs	+	−	−	+	NA	−	−	−	±	NA	NA	NA	NA	● Diabetes	5
4	1012	CoronaVac(Sinovac)	Turkey	HCWs	+	+	NA	NA	NA	NA	NA	NA	NA	NA	NA	NA	NA	NA	6
5	632	BNT162b2(Pfizer–BioNTech)	Italy	Patients: cancer	−	+	+	+	+	NA	NA	NA	NA	NA	NA	NA	● Concomitant disease ● Therapeutic setting ● Active anticancer treatment	● ECOG PS ● Number of metastatic sites ● Type of Metastases	7
6	552	CoronaVac(Sinovac)	UK	Community	+	NA	NA	NA	NA	NA	NA	NA	NA	NA	NA	NA	NA	NA	8
7	548	BNT162b2(Pfizer–BioNTech) or CoronaVac(Sinovac)	Turkey	HCWs	+	−	+	+	NA	NA	NA	NA	NA	NA	NA	NA	● occupation (Medical doctor, Nurse, other healthcare workers) ● Presence of chronic disease (yes or no) ● Pneumococcal vaccine (yes or no)	● smoking (Never,Current,Ever) ● Vaccination status (influenza vaccine)	9
8	539	BNT162b2(Pfizer–BioNTech)	Sweden	Patients: primary immunodeficiency disorders (PID) or human immunodeficiency virus (HIV) , HSCT/chimeric antigen receptor T (CAR T) cell therapy , solid organ transplantation (SOT) , or chronic lymphocytic leukemia (CLL)	−	−	NA	−	NA	NA	NA	NA	NA	NA	NA	NA	● All immunocompromised patients●primary immunodeficiency ● hematopoietic stem cell transplantation ●solid organ transplantation ● chronic lymphocytic leukemia ● Patients goups (HIV vs PID,HSCT,SOT,CLL) ● HSCT-subgroups(Late vs Early) ● HSCT（GvHD absent vs severe) ● SOT(Time to tranplantation,Creatinine baseline, MMF) ● SOT-type of organ(Liver vs Kidney) ● CLL(IgG baseline)● CLL-subgroups(Indolent vs Ibrutinib)	● human immunodeficiency virus ● Lymphocyte count at baseline ● PID(Age,Sex,Co-morbidity, IgG at baseline, Autoimmunity, Malignancy) ● PID-sub group(CVID vs CD4 cytop., Monogenic disease, Other, XLA) ● HSCT-subgroups(Late vs Intermediate) ● HSCT（GvHD absent vs miled,moderate) ● HSCT(Age,Sex,GvHD)● SOT-type of organ(Liver vs Kidney/pancreas) ● SOT(Age,Sex,Tacrolimus) ● CLL(Age,Sex) ● CLL-subgroups(Indolent vs Off ibrutinib, Previous CD20-mAb)	10
9	481	ChAdOx1 nCoV-19(Astra Zeneca) or BBV-152(Bharat Biotech)	India	HCWs	+	−	−	NA	NA	+	NA	−	NA	NA	NA	NA	● Co-morbidities (No co-morbidities vs Any co-morbidities) ● Vaccine type (Vocaxin vs Covaxin) ● Previous infection	● Blood Group ● Type2 Diabetes Mellitus (No vs Yes) ● Duration of T2DM (<5years vs 5-10 years, >10years) ● Dyslipidaemia ● Ischemic Heart Disease	11
10	289	BNT162b2(Pfizer–BioNTech)	Israel	Patients:Dialysis	−	−	NA	NA	NA	NA	NA	NA	NA	+	NA	NA	● dialysis + Post COVID-19 Infection ● Albumin	● hemodialysis ● peritoneal dialysis Diabetes ● Dialysis vintage (dialysis adequacy HD,dialysis adequacy PD)	12
11	276	BNT162b2(Pfizer–BioNTech) or ChAdOx1 nCoV-19(Astra Zeneca)	Greece	Patients: monoclonal gammopathy of undetermined significance (MGUS), smoldering myeloma (SMM)	−	+	−	+	NA	NA	NA	NA	NA	NA	NA	NA	● Multiple myeloma ● treatment type:anti-BCMA-based regimens(belantamab mafodotin and anti-CD38 monoclonal antibodies),anti-CD38-based regimens ● lymphopenia ● low levels of IgA	● MGUS,Smoldering multiple myloma ● International Staging System:ISS(Stage1 vs 2,3) ● Revised International Staging System:RISS(Stage1 vs 2,3) ● Myeloma type(IgG vs IgA,IgM,KLC,LLC) ● low levels of IgM,IgG ● treatment type: PI/IMID-based combinations, Lenalidomide maintenance	13

12	248	BNT162b2(Pfizer–BioNTech)	France	Patients: receiving ICI,patients with pneumonectomy or chronic radiation pneumonitis,patients on oral tyrosine kinase targeted therapy (tyrosine kinase inhibitors [TKIs]); and patients without systemic therapy	+	+	NA	+	+	NA	NA	NA	NA	NA	NA	NA	● chemotherapy,targeted therapy,bevacizumab ● without systemic therapy within 3 months ● single-agent ICI treatment within last 3 months	● chemotherapy vs immunotherapy	14
13	200	BNT162b2(Pfizer–BioNTech)	Japan	Patients: hemodialysis (HD)	+	−	−	NA	NA	+	NA	+	NA	NA	NA	NA	● History of stroke, Dementia ● White blood cell count	● Creatinine ● Blood urea nitrogen ● Hemoglobin ● White blood cell count ● Mean KT/V ● Dialysis mellitus	15
14	200	BNT162b2(Pfizer–BioNTech)	Denmark	Patients: solid organ transplant (SOT) recipients	+	−	−	±	NA	NA	NA	+	NA	NA	NA	NA	● Transplanted <1 year before vaccination ● Immunosuppressive treatment (Corticosteroids) ● Type of organ transplanted (Liver vs Kidney, Lung) ● Comorbidities (Diabetes mellitus, De novo non-skin cancer)	● Immunosuppressive (No antimetabolite vs Azathioprine,Mycophenolate)● Immunosuppressive(Calcineurin inhibitor vs mTOR inhibitor) ● Comorbidities(Chronic pulmonary disease)	16
15	194	BNT162b2(Pfizer–BioNTech) or mRNA-1273(Moderna)	Switzerland	Patients: allogeneic hematopoietic cell transplantation (allo-HCT) graft-versus-host disease (GVHD)	+	−	NA	NA	NA	NA	NA	NA	NA	NA	NA	NA	● IST ● underlying disease ● allo-HCT resipients ● preinfection	● chronic GVHD	17
16	185	CoronaVac(Sinovac)	Thailand	HCWs	+	−	NA	NA	NA	NA	NA	NA	NA	NA	NA	NA	NA	● occupation	18
17	156	BNT162b2(Pfizer–BioNTech)	Portugal	Patients: hemodialysis (HD)	+	−	−	−	−	−	NA	−	NA	+	NA	NA	● Leukemia	● Laboratory parameters (Hemoglobin, Serum slbumin, Ferritin, nPCR, CRP,25(OH) D3) ● Comorbidities (Diabetes mellitus, Chronic liver disease, Rheumatic disease, Past Kidney transplant) ● Medication (Erythropoiesis-stimulating agent,Angiotensin-converting-enzyme inhibitor,Statins,Corticosteroid,Other immunossupressor/immunomodulator,Tacrolimus,Non-steroidal anti-inflammatory drug,Antithrombotic,Anti-HBc positivity)	19
18	155	CoronaVac(Sinovac)	Turkey	Patients: kidney transplant recipients (KTRs) and hemodialysis (HD)	+	NA	−	NA	NA	NA	NA	NA	NA	NA	NA	NA	NA	● Absolute lymphocyte count ● Neutrophil lymphocyte ratio ● 25-OH-vitamin D3	20
19	150	BNT162b2(Pfizer–BioNTech)	Netherlands	Patients: previously SARS-CoV-2-infected	−	±	NA	NA	NA	NA	NA	NA	NA	NA	NA	NA	● illness on set dating >1 year before vaccination ● severe disease outcomes	NA	21
20	142	BNT162b2(Pfizer–BioNTech)	Canada	Patients: receiving in-center hemodialysis	−	−	NA	NA	NA	NA	NA	NA	NA	+	NA	NA	NA	NA	22
21	136	BNT162b2(Pfizer–BioNTech)	France	Patients: rheumatic and musculoskeletal	−	−	NA	NA	−	NA	NA	NA	NA	NA	NA	NA	● Mycophenolate ● Methotrexate	● At least one BILAG score ≥B ● C3, g/L ● dsDNA antibodies, IU/mL ● Detectable IFN-α ● Total	23

				diseases (RMDs) and associated immune-modulatory treatments														serum IgA, g/L ● Total serum IgM, g/L ● Lymphocytes count, G/L● Hydroxychloroquine ● Azathioprine ● Belimumab ● Other immunosuppressor	
22	136	BNT162b2(Pfizer–BioNTech) or CoronaVac(Sinovac) or ChAdOx1 nCoV-19(Astra Zeneca) or Ad26.COV2.S(Janssen)	Portugal	HCWs	−	−	NA	NA	NA	NA	NA	NA	NA	NA	NA	NA	NA	● Vaccine reactogenicity	24
23	126	BNT162b2(Pfizer–BioNTech)	Germany	HCWs	NA	NA	NA	NA	NA	NA	NA	NA	NA	NA	NA	NA	NA	● Selenium (Se) supplementation	25
24	110	BNT162b2(Pfizer–BioNTech) or ChAdOx1 nCoV-19(Astra Zeneca) or mRNA-1273(Moderna)	France	HCWs	+	−	−	NA	NA	NA	NA	NA	NA	NA	NA	NA	NA	● Comorbidity	26
25	109	BNT162b2(Pfizer–BioNTech)	Finland	Patients: multiple myeloma (MM) and myeloproliferative malignancies (MPM)	−	−	−	+	NA	NA	NA	NA	NA	NA	NA	NA	NA	● multiple myeloma (MM) ● myeloproliferative malignancies (MPM) ●Treatment (Daratumumab-based vs PI-based/Imids-based alone or in combo without daratumumab)	● Lines of therapy ● Lymphocyte count ● Time from diagnosis to vaccination	27
26	103	BNT162b2(Pfizer–BioNTech)	U.S.	Patients: solid tumors	NA	NA	NA	−	NA	NA	NA	NA	NA	NA	NA	NA	NA	● cancer	NA	28
27	100	CoronaVac(Sinovac)	China	HCWs	+	−	NA	NA	NA	NA	NA	NA	NA	NA	NA	NA	NA	● interval between two doses	NA	29
28	75	BBIBP-CorV(Sinopharm)	China	community	+	NA	+	NA	NA	NA	NA	NA	NA	NA	NA	NA	NA	● absolute lymphocyte count ● high levels of serum SAA (serum amyloid A) ● low T3 before vaccination ● Higher levels of absolute lymphocyte count accompanied by lower serum SAA	● biochemical routine indexes (blood cell counts and differentials,ALT,AST,GGT,CHE, ALP,TBA,LDH,CRP) ●thyroid function markers except T3 ● comorbidities	30
29	49	BNT162b2(Pfizer–BioNTech)	Japan	HCWs	+	−	NA	NA	NA	NA	NA	NA	NA	NA	NA	NA	+	● alchol drinking habits	● Smoking habits ● Allergies ● Other side effects after vaccination	31
30	44	BNT162b2(Pfizer–BioNTech)	Italy	Patients: chemotherapy	+	NA	±	NA	NA	NA	NA	NA	NA	NA	NA	NA	NA	NA	● oncology(After 1 months) ● Comorbidity ● Progressive disease ● Chemotherapy in progress ● FIGO stage	32
31	43	BNT162b2(Pfizer–BioNTech)	Germany	Patients: dialysis	NA	NA	NA	NA	NA	NA	NA	NA	NA	NA	+	NA	NA	● oncology(After 3 months)	NA	33
32	41	BNT162b2(Pfizer–BioNTech)	Japan	Patients: solid tumors	NA	NA	NA	+	NA	NA	NA	NA	NA	NA	NA	NA	NA	● cytotoxic chemotherapy ● immune checkpoint inhibitors	● cytotoxic chemotherapy vs immune checkpoint inhibitors	34
33	40	BNT162b2(Pfizer–BioNTech) or mRNA-1273(Moderna)	U.S.	HCWs	NA	−	NA	NA	NA	NA	NA	NA	NA	NA	NA	NA	NA	● Previous infection	NA	35
34	29	BNT162b2(Pfizer–BioNTech)	Israel	Patients: primary brain tumors	−	+	NA	NA	+	NA	NA	NA	NA	NA	NA	NA	NA	● primary brain tumors (PBTs)	● Treatments (Surgery,Temozolomide,Elapsed time from vaccination) ● Diagnosis(Artypical meningioma, Glioblastoma multiforme, Oligodendroglioma)	37

Supplementary Table 4. Estimated fixed and individual parameters for 12 health care workers

Parameter or variable	Decay rate of antibody-secreting cells	Maximum *de novo* production of antibody by 1st vaccination	Delay of antibody-secreting cells induction after 1st vaccination.	Steepness at which induction increases with increasing the amount of mRNA	Amount of mRNA satisfying $P_i/2$	Maximum *de novo* production of antibody by 2nd vaccination	Delay of antibody-secreting cells induction after 2nd vaccination.
Symbol	μ	H_1	η_1	m	K	H_2	η_2
Unit	day^{-1}	AU/mL	day	---	$\mu g/0.5\mathrm{mL}$	AU/mL	day
Individual estimated parameters for $S1$ to $S12$							
$S1$	0.885346	650.518	12.5269	0.0373144	33900	5227.34	4.21433
$S2$	0.885346	760.114	12.5109	0.028673	33900	5035.79	4.23423
$S3$	0.885346	2375.11	12.5096	0.0223842	33900	7562.82	3.85759
$S4$	0.885346	790.745	12.4927	0.0611514	33900	7304.66	3.95306
$S5$	0.885346	942.686	12.5169	0.0250174	33900	5638.12	3.91276
$S6$	0.885346	448.87	12.5243	0.0851651	33900	3828.1	4.24752
$S7$	0.885346	1848.01	12.5471	0.0272096	33900	9073.94	4.2513
$S8$	0.885346	567.839	12.5409	0.0523284	33900	4673.2	4.71178
$S9$	0.885346	1835.9	12.5428	0.0365247	33900	7517.48	4.59114
$S10$	0.885346	1201.77	12.5109	0.0625655	33900	5916.28	4.17894
$S11$	0.885346	736.229	12.5086	0.0700219	33900	4118.67	4.54006
$S12$	0.885346	1369.65	12.5409	0.0488345	33900	8226.08	4.23969
Population estimated parameters							
−−−	0.885346	975.297	12.52	0.0437653	33900	6035.142	4.25

Supplementary Note 1: **Literature review**

This comprehensive literature review aimed to characterize the Fukushima vaccination cohort from previous cohort studies and to identify the factors contributing to the vulnerability of certain populations. A total of 440 articles published up to March 23, 2022, were collected using PubMed. Details of the search terms used in this analysis are provided in **Supplementary Table 1**. In the first step, a group of two or three authors (YT, MK, MY, TA, YS) screened and retrieved articles according to the following two criteria: (i) report evaluating antibody titer testing of human blood samples after two doses of SARS-CoV-2 vaccine; (ii) report collecting at least two blood samples after two doses of SARS-CoV-2 vaccine, and 92 articles met the criteria. **Fig 1F** shows the overall distribution of the cohort size and study period of the included papers. *Study period* was defined as the maximum period between the first vaccination and the completion of the last sampling, and *cohort size* was defined as the maximum number of participants who had at least one sample collected at certain sampling times during the period. The median cohort size was 103 and the median study period was 150 days, and six articles were found to have a cohort size of 1,000 or more (**Supplementary Table 2**). Next, we extracted and analyzed the factors contributing to vulnerable population status from 40 of 92 papers, including interview sheets, 6 of which were excluded because they did not analyze factors of vulnerability (**Supplementary Table 3**). From this literature review, we found that only the Fukushima cohort (1) consecutively sampled more than 2,000 of the same individuals with less dropout (only 3.3%); (2) included an interview sheet for all participants; (3) targeted “communities” (including non-HCWs); and (4) measured several modalities of antibody titers including neutralizing activity (**Supplementary Table 2**).

Supplementary Note 2: **Stratifying time-course pattern of antibody dynamics**

For the purpose of stratification of the individual vaccine-elicited antibody response, we first applied unsupervised random forest clustering to the individual "reconstructed" antibody dynamics of 2,407 participants (e.g., **Supplementary Fig 2**) but failed to divide the time-course pattern of antibody dynamics into different clusters (data not shown). To overcome this problem, we employed an idea of "feature engineering": extracting features to improve the quality of results from a machine-learning process, compared with supplying only the raw data to it. We quantified the peak, duration, and area under the curve of the reconstructed antibody dynamics as their features (**Extended Data Fig 5D**). Interestingly, the unsupervised random forest clustering based on these features in addition to our estimated individual parameters (i.e., m and H_2) identified 10 clusters that clearly discriminated the time-course patterns (**Extended Data Fig 2AB**). Since the time-course patterns of clusters 2, 3, 6, and 7 were similar and they were close together in two-dimensional Uniform Manifold Approximation and Projection (UMAP) embeddings (**Extended Data Fig 2A**), we merged these clusters into one group. In addition, we removed cluster 8 from further evaluation (i.e., we removed 245 individuals, around 10%, of the 2,407 participants in the Fukushima cohort) on the grounds that their reconstructed antibody dynamics with estimated parameters may not be reasonable. This is because their antibody titers measured from two blood samples showed statistically significantly small differences ($p < 1.0 \times 10^{-16}$ by Welch two sample t-test) and their sampling intervals were significantly shorter than the others ($p = 0.01$ by Welch two sample t-test) (**Extended Data Fig 2C**). This problem will be solved by adjusting for the timing of their blood sampling in our future study of booster vaccinations. Finally, we obtained 6 groups to evaluate the stratification in further detail (**Fig 2A**).

Supplementary Note 3: **Inter-relationship of various features**

We visualized the inter-relationship of various features using principal component analysis (PCA) based on their correlation matrix (**Fig 3F** and **Extended Data Fig 3C**). We found that the first principal axis, explaining 25.9% of the variance, represents titers: the antibody titers and the dynamic parameters of each individual (i.e., their peak, duration, and area under the curve, m and H_2) were located in the third quadrant of this PCA plane. The adverse events were in the second quadrant, suggesting their closeness to high antibody titers. However, most questionnaire items about basic demographic information and lifestyle habits remained in the middle, indicating their relatively minor role. A notable exception was age, which was inversely correlated with titers and was indeed situated in the fourth quadrant. By contrast, the second principal axis, explaining 9.8% of the variance, represents comorbidities and medication. Our stratification combines these information and places G1, G2, and G4 in the third quadrant; G3 in the middle; and G5 and G6 in the fourth quadrant near the comorbidities cluster and age.

References

1. Levin, E.G.*, et al.* Waning Immune Humoral Response to BNT162b2 Covid-19 Vaccine over 6 Months. *N Engl J Med* **385**, e84 (2021).
2. Papadopoli, R.*, et al.* Serological Response to SARS-CoV-2 Messenger RNA Vaccine: Real-World Evidence from Italian Adult Population. *Vaccines (Basel)* **9**(2021).
3. Buonfrate, D.*, et al.* Antibody response induced by the BNT162b2 mRNA COVID-19 vaccine in a cohort of health-care workers, with or without prior SARS-CoV-2 infection: a prospective study. *Clin Microbiol Infect* **27**, 1845-1850 (2021).
4. Shachor-Meyouhas, Y.*, et al.* Immunogenicity trends 1 and 3 months after second BNT162B2 vaccination among healthcare workers in Israel. *Clin Microbiol Infect* **28**, 450 e451-450 e454 (2022).
5. Lustig, Y.*, et al.* BNT162b2 COVID-19 vaccine and correlates of humoral immune responses and dynamics: a prospective, single-centre, longitudinal cohort study in health-care workers. *Lancet Respir Med* **9**, 999-1009 (2021).
6. Demirbakan, H., Kocer, I., Erdogan, M. & Bayram, A. Assessing humoral immune response after two doses of an inactivated SARS-CoV-2 vaccine (CoronaVac) in healthcare workers. *Public Health* **205**, 1-5 (2022).
7. Di Noia, V.*, et al.* Rapid decline of humoral response to two doses of BNT162b2 vaccine in patients with solid cancer after six months: The urgent need of the additional dose! *Eur J Cancer* **165**, 169-173 (2022).
8. Ramasamy, M.N.*, et al.* Safety and immunogenicity of ChAdOx1 nCoV-19 vaccine administered in a prime-boost regimen in young and old adults (COV002): a single-blind, randomised, controlled, phase 2/3 trial. *Lancet* **396**, 1979-1993 (2021).
9. Caglayan, D.*, et al.* An analysis of antibody response following the second dose of CoronaVac and humoral response after booster dose with BNT162b2 or CoronaVac among healthcare workers in Turkey. *J Med Virol* **94**, 2212-2221 (2022).
10. Bergman, P.*, et al.* Safety and efficacy of the mRNA BNT162b2 vaccine against SARS-CoV-2 in five groups of immunocompromised patients and healthy controls in a prospective open-label clinical trial. *EBioMedicine* **74**, 103705 (2021).
11. Singh, A.K.*, et al.* Humoral antibody kinetics with ChAdOx1-nCOV (Covishield) and BBV-152 (Covaxin) vaccine among Indian Healthcare workers: A 6-month longitudinal cross-sectional Coronavirus Vaccine-induced antibody titre (COVAT) study. *Diabetes Metab Syndr* **16**, 102424 (2022).
12. Berar-Yanay, N.*, et al.* Waning Humoral Response 3 to 6 Months after Vaccination with the SARS-COV-2 BNT162b2 mRNA Vaccine in Dialysis Patients. *J Clin Med* **11**(2021).
13. Terpos, E.*, et al.* The neutralizing antibody response post COVID-19 vaccination in patients with myeloma is highly dependent on the type of anti-myeloma treatment. *Blood Cancer J* **11**, 138 (2021).
14. Gounant, V.*, et al.* Efficacy of Severe Acute Respiratory Syndrome Coronavirus-2 Vaccine in Patients With Thoracic Cancer: A Prospective Study Supporting a Third Dose in Patients With Minimal Serologic Response After Two Vaccine Doses. *J Thorac Oncol* **17**, 239-251 (2022).
15. Kitamura, M.*, et al.* Low humoral immune response to the BNT162b2 vaccine against COVID-19 in nursing home residents undergoing hemodialysis: a case-control observational study. *Ren Replace Ther* **8**, 8 (2022).
16. Hamm, S.R.*, et al.* Decline in Antibody Concentration 6 Months After Two Doses of SARS-CoV-2 BNT162b2 Vaccine in Solid Organ Transplant Recipients and Healthy Controls. *Front Immunol* **13**, 832501 (2022).

17. Huang, A.*, et al.* Antibody Response to SARS-CoV-2 Vaccination in Patients following Allogeneic Hematopoietic Cell Transplantation. *Transplant Cell Ther* **28**, 214 e211-214 e211 (2022).
18. Benjamanukul, S.*, et al.* Safety and immunogenicity of inactivated COVID-19 vaccine in health care workers. *J Med Virol* **94**, 1442-1449 (2022).
19. Weigert, A.*, et al.* Longitudinal Analysis of Antibody Responses to the mRNA BNT162b2 Vaccine in Patients Undergoing Maintenance Hemodialysis: A 6-Month Follow-Up. *Front Med (Lausanne)* **8**, 796676 (2021).
20. Dheir, H.*, et al.* Short and mid-term SARS-CoV-2 antibody response after inactivated COVID-19 vaccine in hemodialysis and kidney transplant patients. *J Med Virol* (2022).
21. van Gils, M.J.*, et al.* A single mRNA vaccine dose in COVID-19 patients boosts neutralizing antibodies against SARS-CoV-2 and variants of concern. *Cell Rep Med* **3**, 100486 (2022).
22. Yau, K.*, et al.* Evaluation of the SARS-CoV-2 Antibody Response to the BNT162b2 Vaccine in Patients Undergoing Hemodialysis. *JAMA Netw Open* **4**, e2123622 (2021).
23. Moyon, Q.*, et al.* BNT162b2 vaccine-induced humoral and cellular responses against SARS-CoV-2 variants in systemic lupus erythematosus. *Ann Rheum Dis* **81**, 575-583 (2022).
24. Guiomar, R.*, et al.* Monitoring of SARS-CoV-2 Specific Antibodies after Vaccination. *Vaccines (Basel)* **10**(2022).
25. Demircan, K.*, et al.* Humoral immune response to COVID-19 mRNA vaccination in relation to selenium status. *Redox Biol* **50**, 102242 (2022).
26. Bonnet, B.*, et al.* Decline of Humoral and Cellular Immune Responses Against SARS-CoV-2 6 Months After Full BNT162b2 Vaccination in Hospital Healthcare Workers. *Front Immunol* **13**, 842912 (2022).
27. Pimpinelli, F.*, et al.* Fifth-week immunogenicity and safety of anti-SARS-CoV-2 BNT162b2 vaccine in patients with multiple myeloma and myeloproliferative malignancies on active treatment: preliminary data from a single institution. *J Hematol Oncol* **14**, 81 (2021).
28. Shroff, R.T.*, et al.* Immune responses to two and three doses of the BNT162b2 mRNA vaccine in adults with solid tumors. *Nat Med* **27**, 2002-2011 (2021).
29. Chen, Y.*, et al.* Dynamic SARS-CoV-2-specific B-cell and T-cell responses following immunization with an inactivated COVID-19 vaccine. *Clin Microbiol Infect* **28**, 410-418 (2022).
30. Zhang, J.*, et al.* Differential Antibody Response to Inactivated COVID-19 Vaccines in Healthy Subjects. *Front Cell Infect Microbiol* **11**, 791660 (2021).
31. Ikezaki, H., Nomura, H. & Shimono, N. Dynamics of anti-Spike IgG antibody level after the second BNT162b2 COVID-19 vaccination in health care workers. *J Infect Chemother* (2022).
32. Palaia, I.*, et al.* Pfizer-BioNTech COVID-19 Vaccine in Gynecologic Oncology Patients: A Prospective Cohort Study. *Vaccines (Basel)* **10**(2021).
33. Schrezenmeier, E.*, et al.* Immunogenicity of COVID-19 Tozinameran Vaccination in Patients on Chronic Dialysis. *Front Immunol* **12**, 690698 (2021).
34. Funakoshi, Y.*, et al.* Safety and immunogenicity of the COVID-19 vaccine BNT162b2 in patients undergoing chemotherapy for solid cancer. *J Infect Chemother* **28**, 516-520 (2022).
35. Lucas, C.*, et al.* Impact of circulating SARS-CoV-2 variants on mRNA vaccine-induced immunity. *Nature* **600**, 523-529 (2021).
36. Beilhack, G.*, et al.* Antibody Response and Safety After mRNA-1273 SARS-CoV-2 Vaccination in Peritoneal Dialysis Patients - the Vienna Cohort. *Front Immunol* **12**, 780594 (2021).
37. Massarweh, A.*, et al.* Immunogenicity of the BNT162b2 mRNA COVID-19 vaccine in patients with primary brain tumors: a prospective cohort study. *J Neurooncol* **156**, 483-489 (2022).

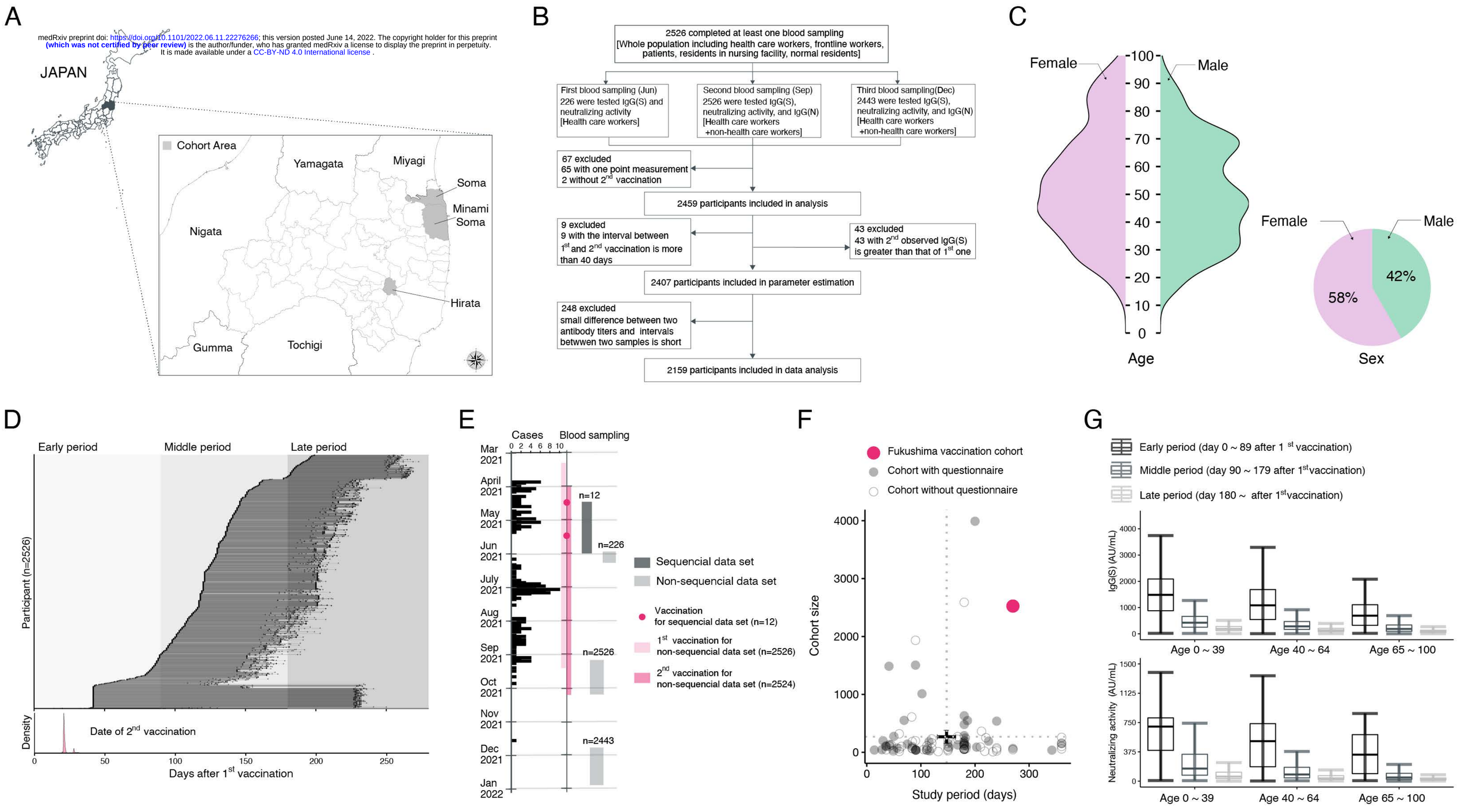

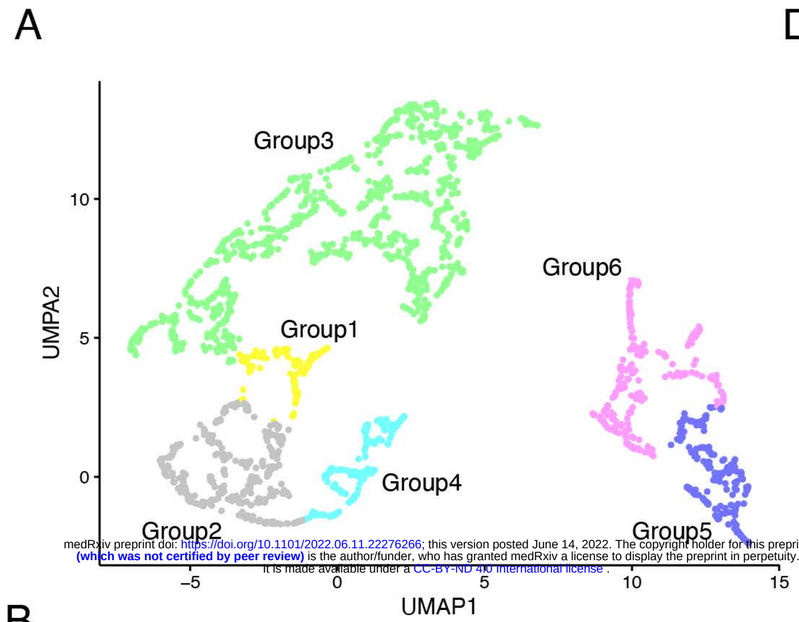

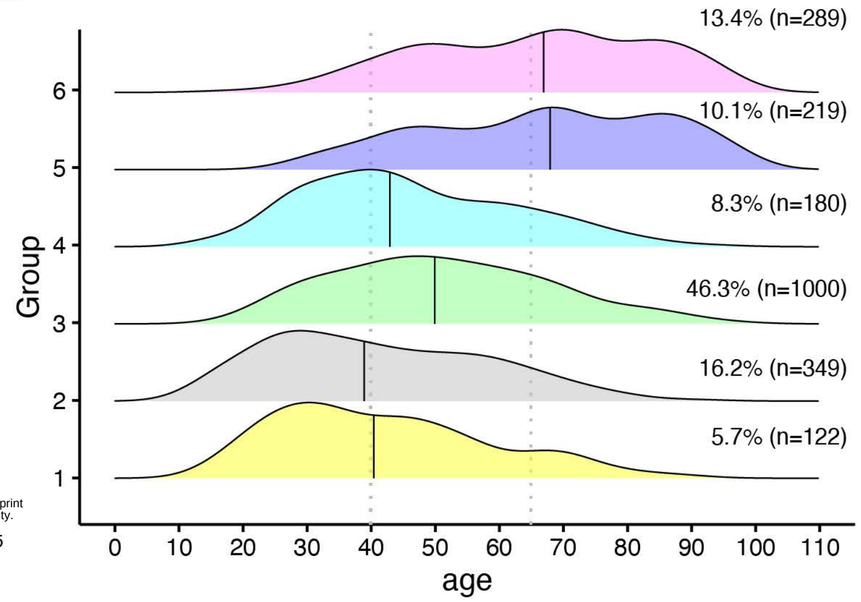

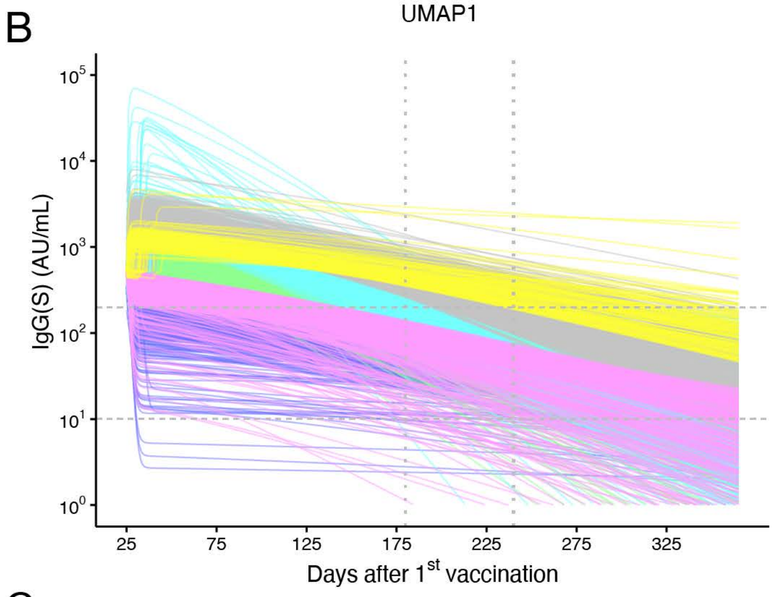

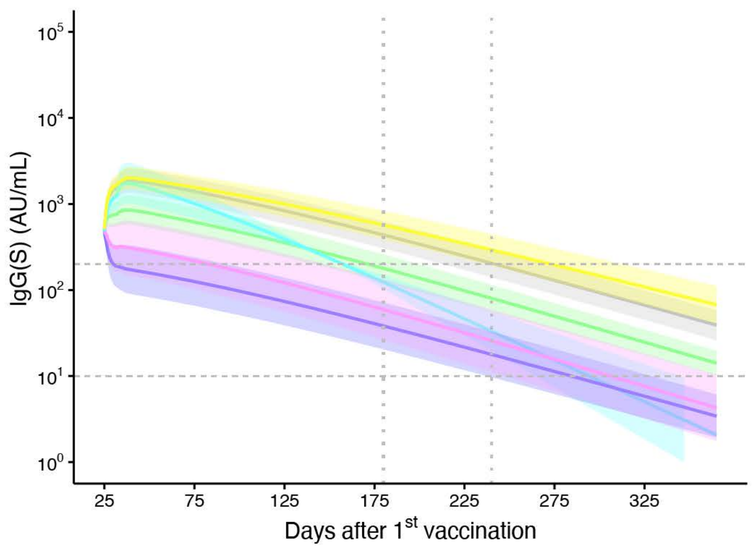

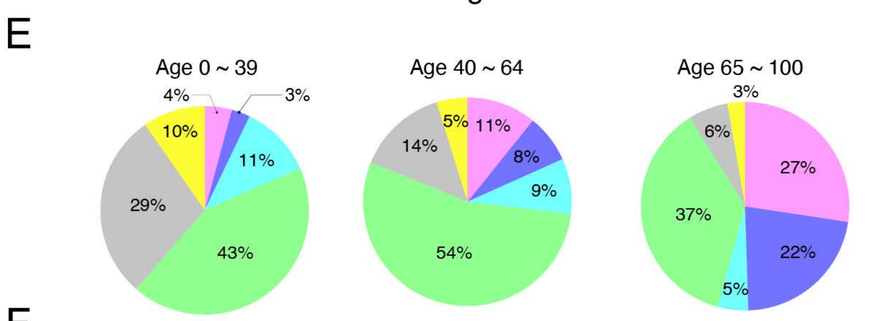

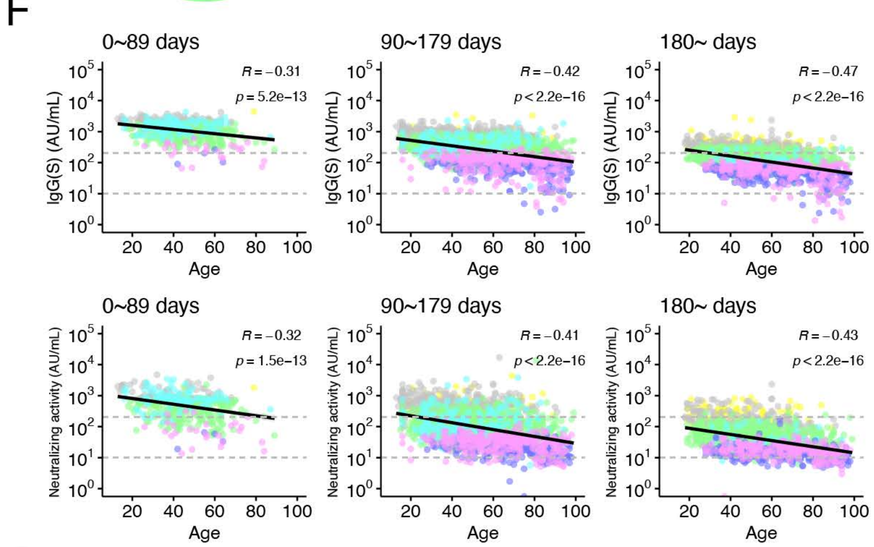

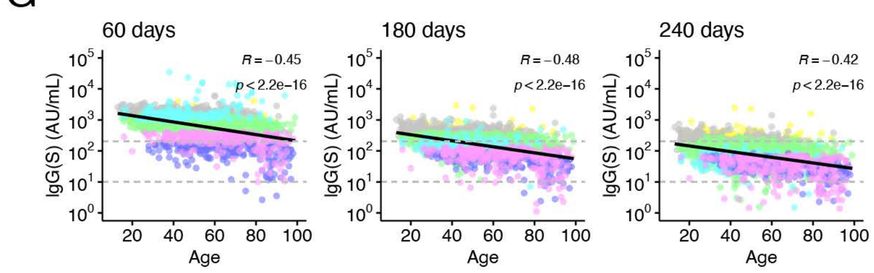

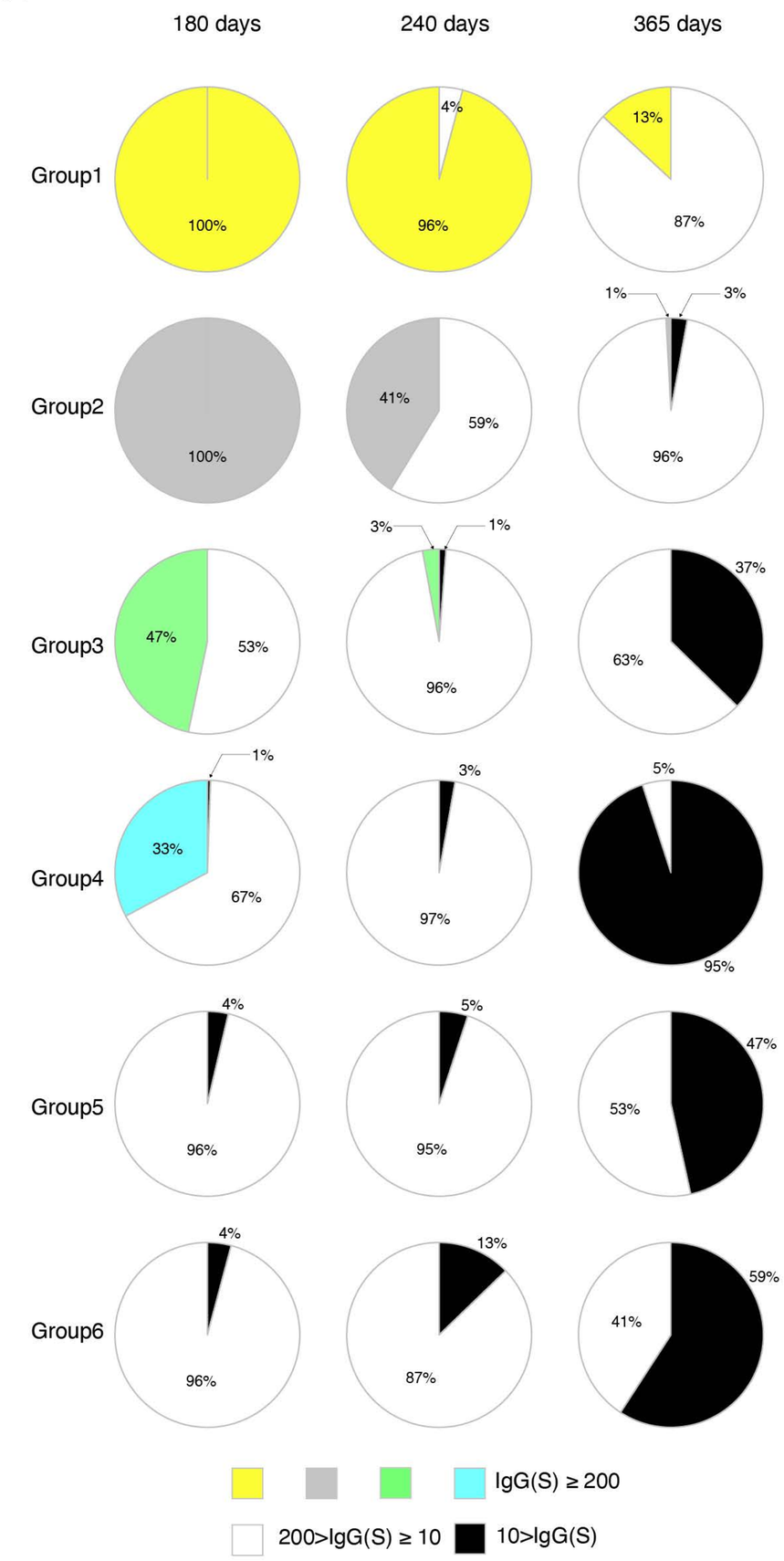

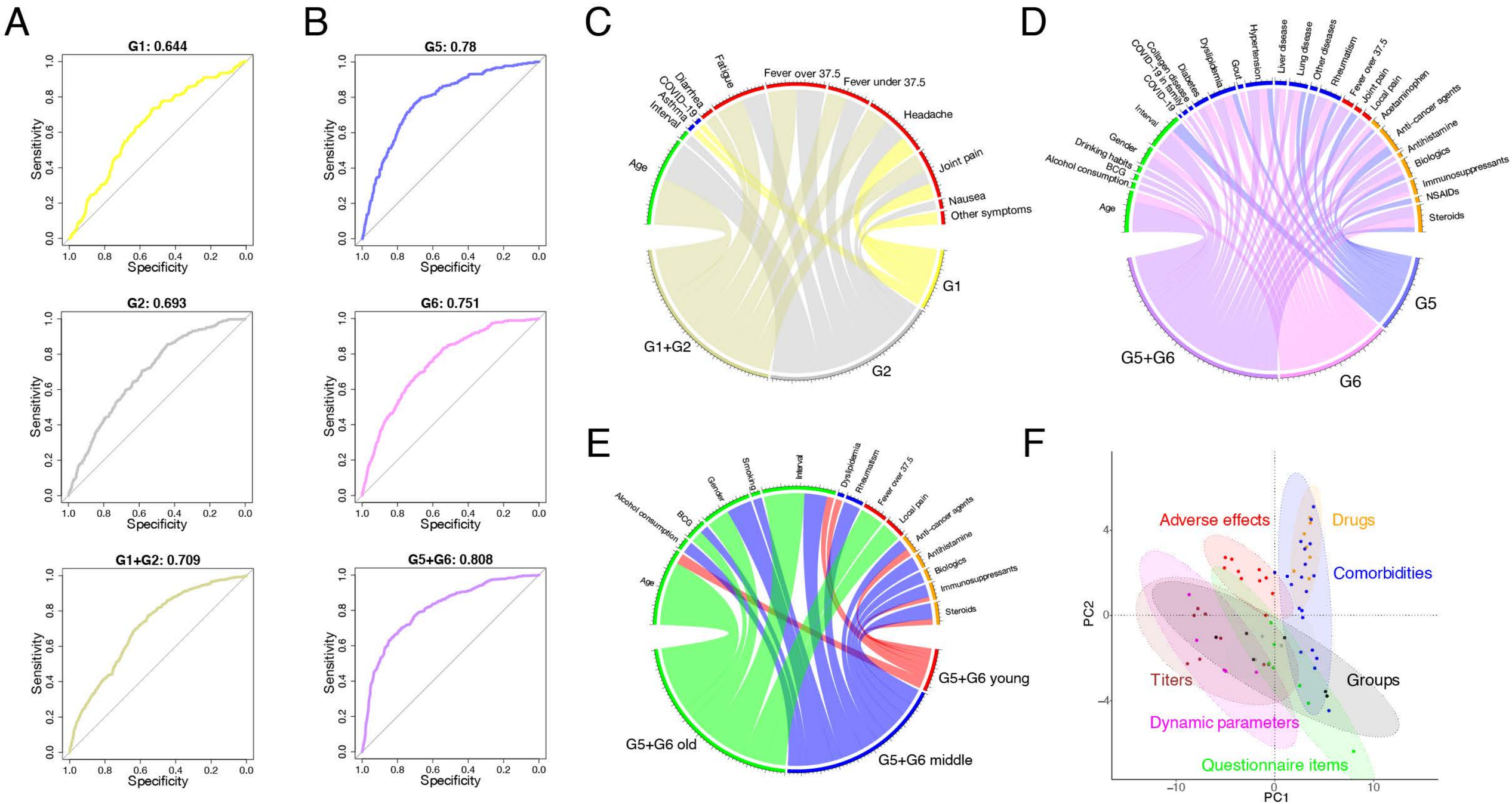
A
G1: 0.644
G2: 0.693
G1+G2: 0.709
B
G5: 0.78
G6: 0.751
G5+G6: 0.808
Sensitivity
Specificity
C
Fever over 37.5
Fever under 37.5
Headache
Joint pain
Nausea
Other symptoms
Fatigue
Diarrhea
COVID-19
Asthma
Interval
Age
G1
G2
G1+G2
D
Hypertension
Liver disease
Lung disease
Other diseases
Rheumatism
Fever over 37.5
Joint pain
Local pain
Acetaminophen
Anti-cancer agents
Antihistamine
Biologics
Immunosuppressants
NSAIDs
Steroids
Dyslipidemia
Gout
Diabetes
Collagen disease
COVID-19 in family
COVID-19
Interval
Gender
Drinking habits
BCG
Alcohol consumption
Age
G5
G6
G5+G6
E
Dyslipidemia
Rheumatism
Fever over 37.5
Local pain
Anti-cancer agents
Antihistamine
Biologics
Immunosuppressants
Steroids
Smoking
Interval
Gender
BCG
Alcohol consumption
Age
G5+G6 young
G5+G6 middle
G5+G6 old
F
Adverse effects
Drugs
Comorbidities
Titers
Groups
Dynamic parameters
Questionnaire items
PC1
PC2

A

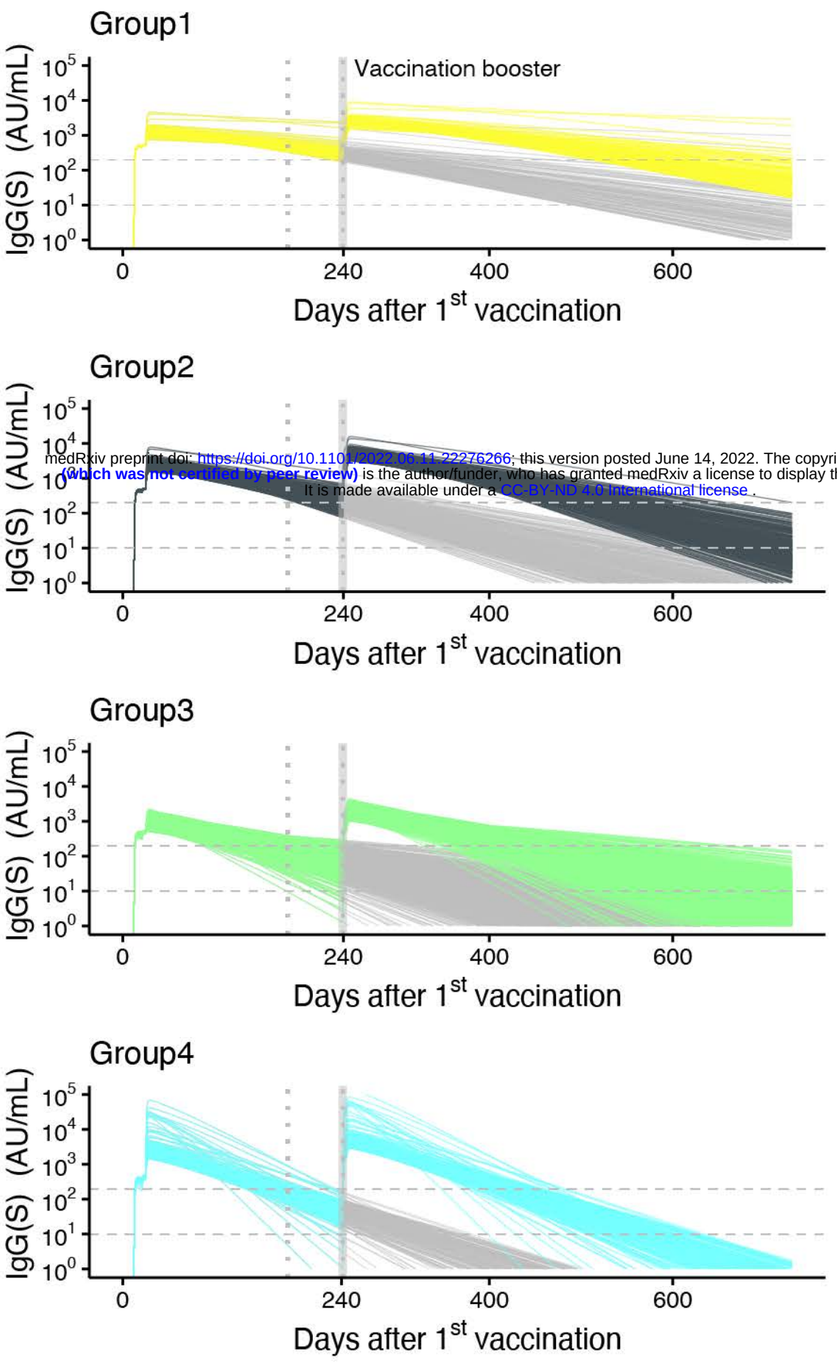

B

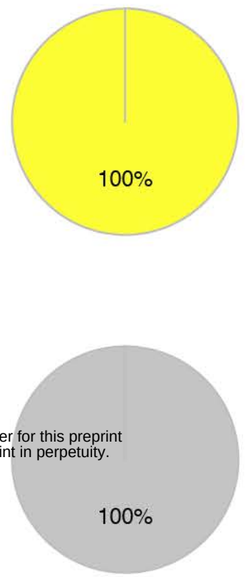

C

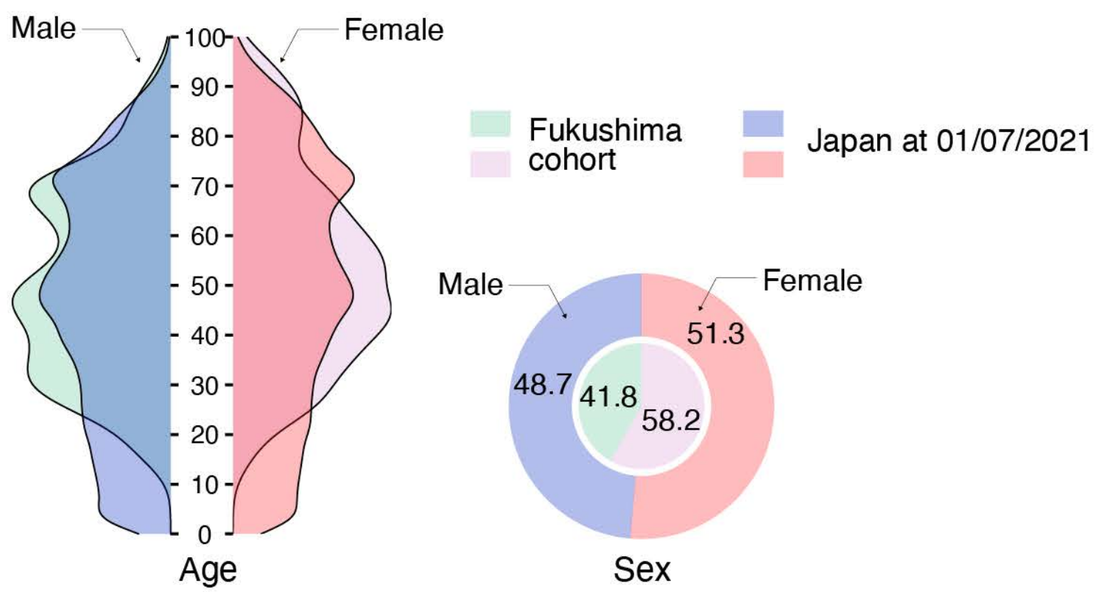

D

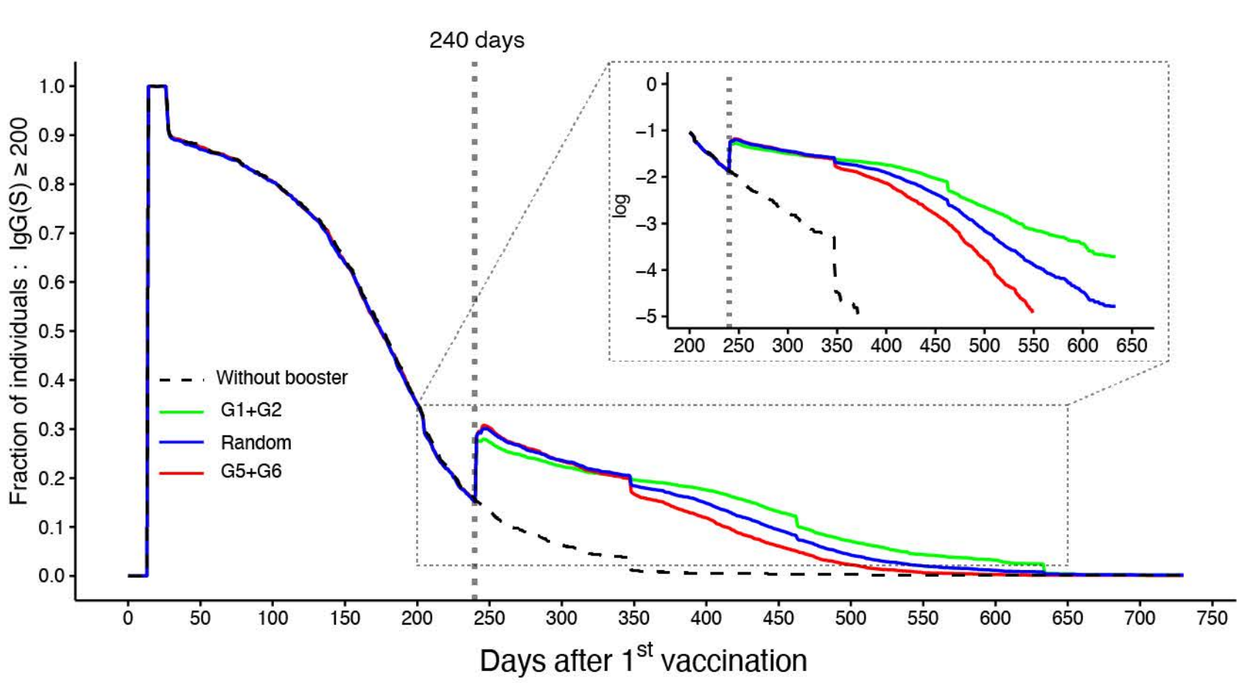

E

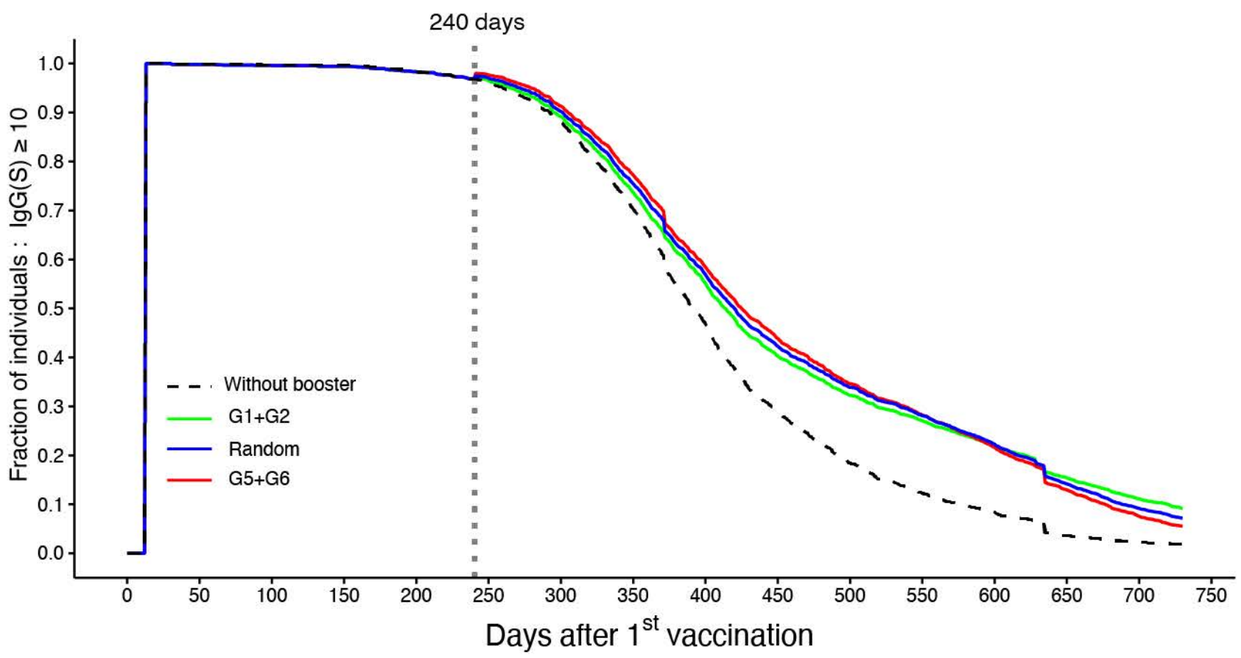

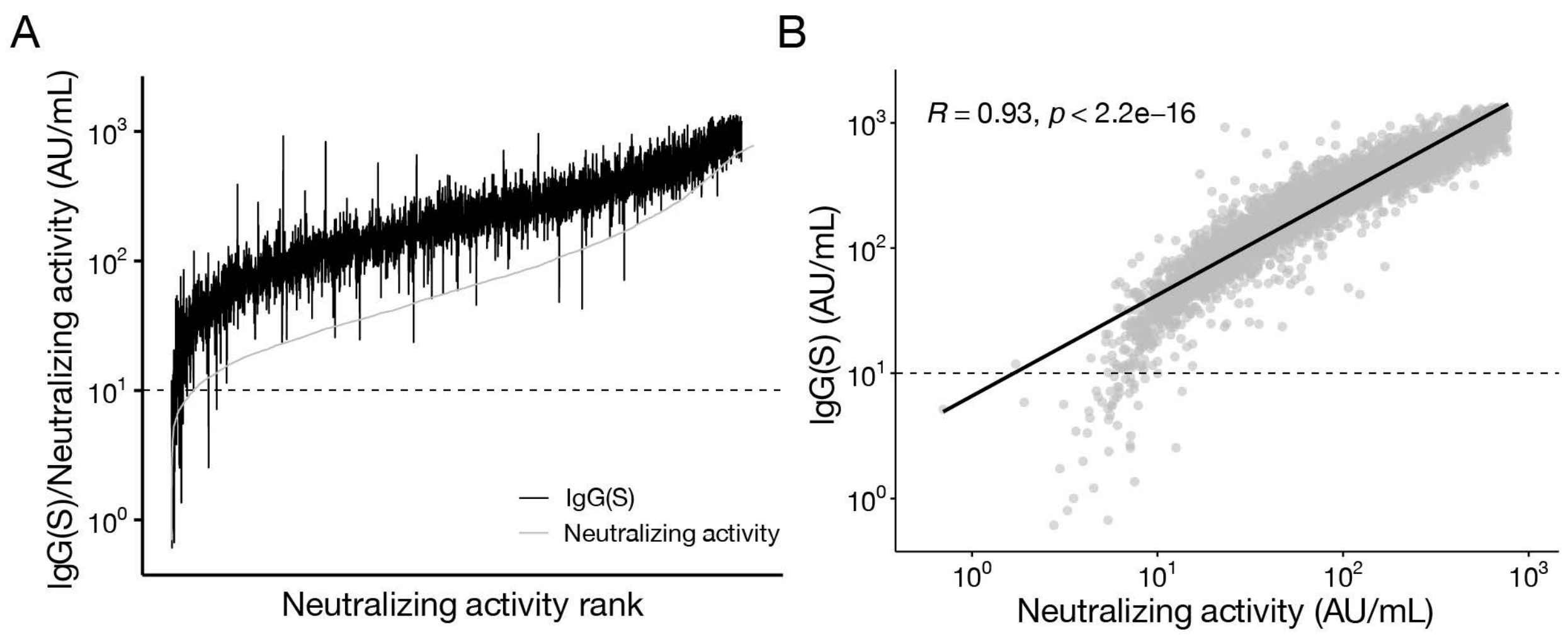
A
IgG(S)/Neutralizing activity (AU/mL)
10^3
10^2
10^1
10^0
IgG(S)
Neutralizing activity
Neutralizing activity rank
B
$R = 0.93$, $p < 2.2e{-}16$
IgG(S) (AU/mL)
10^3
10^2
10^1
10^0
10^0
10^1
10^2
10^3
Neutralizing activity (AU/mL)

A

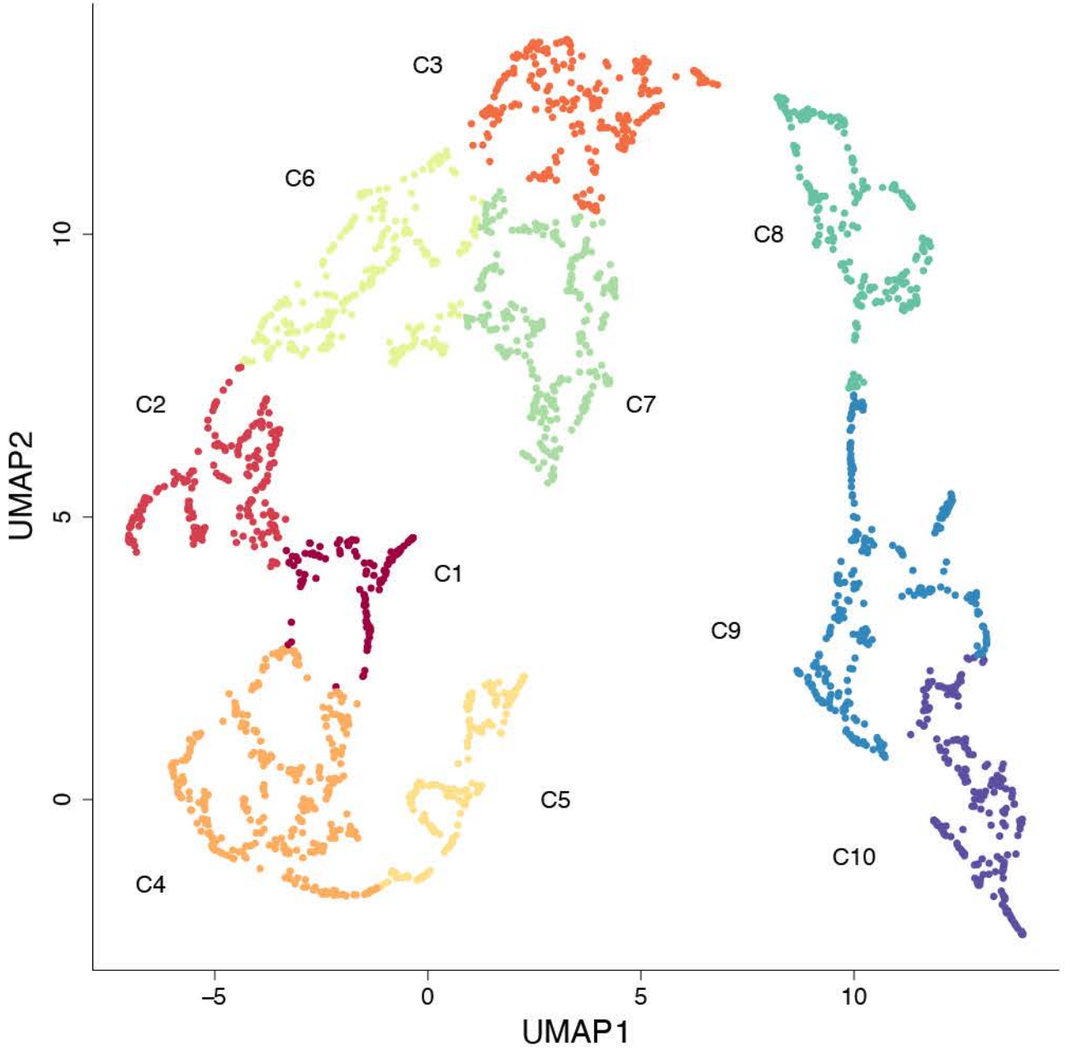
C3
C6
C8
C2
C7
C1
C9
C5
C10
C4
UMAP2
UMAP1
10
5
0
−5
0
5
10

B

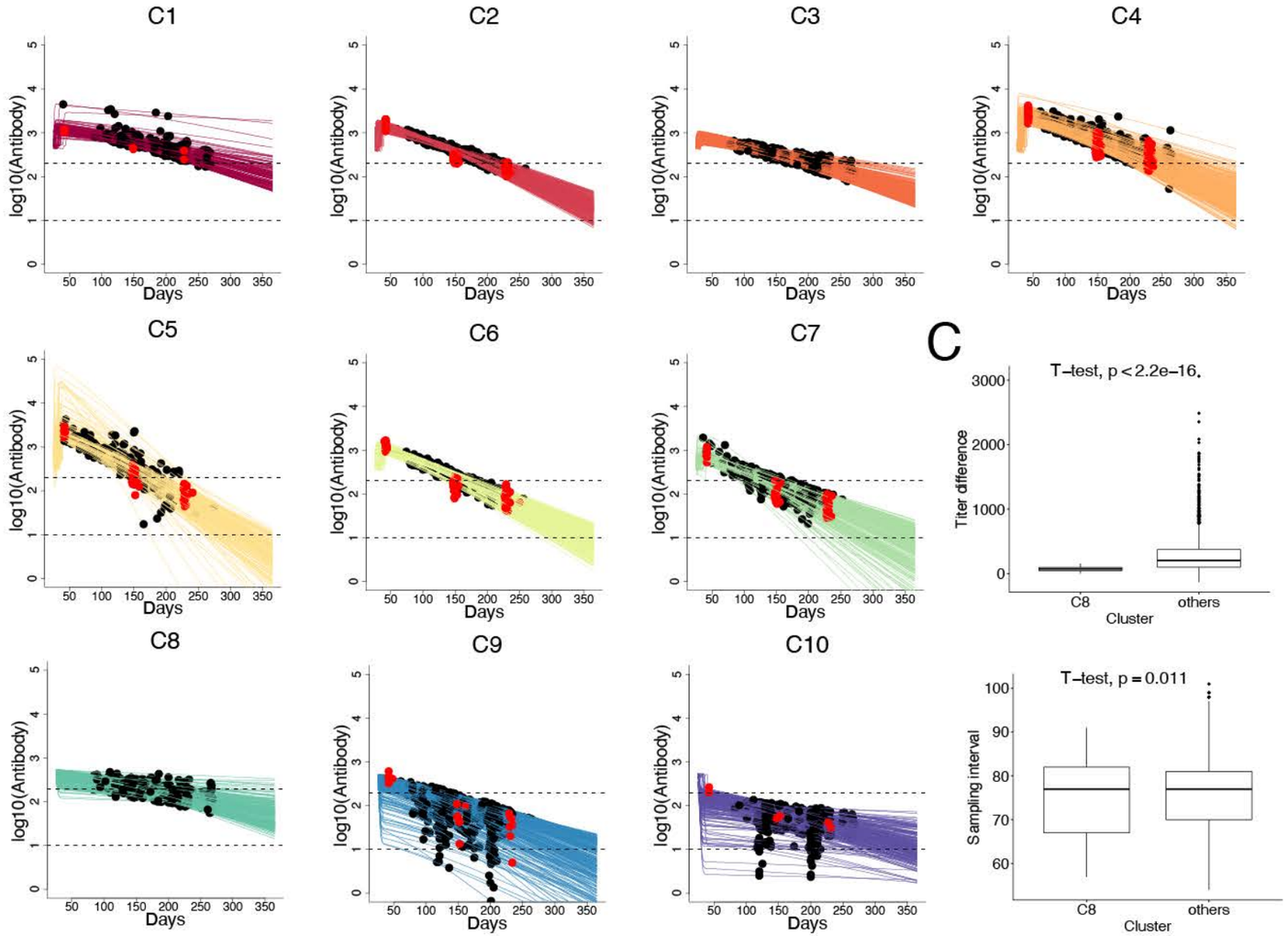
C1
C2
C3
C4
C5
C6
C7
C8
C9
C10
log10(Antibody)
Days

C

T–test, p < 2.2e–16.
Titer difference
C8
others
Cluster

T–test, p = 0.011
Sampling interval
C8
others
Cluster

D

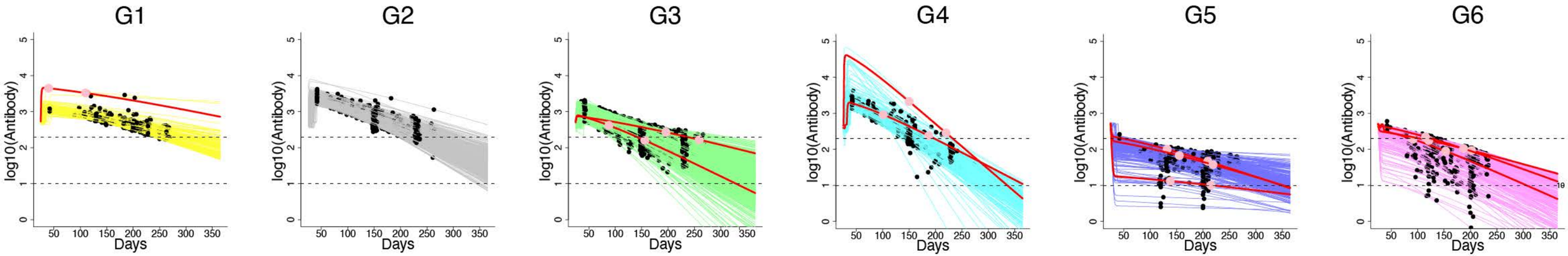
G1
G2
G3
G4
G5
G6
log10(Antibody)
Days

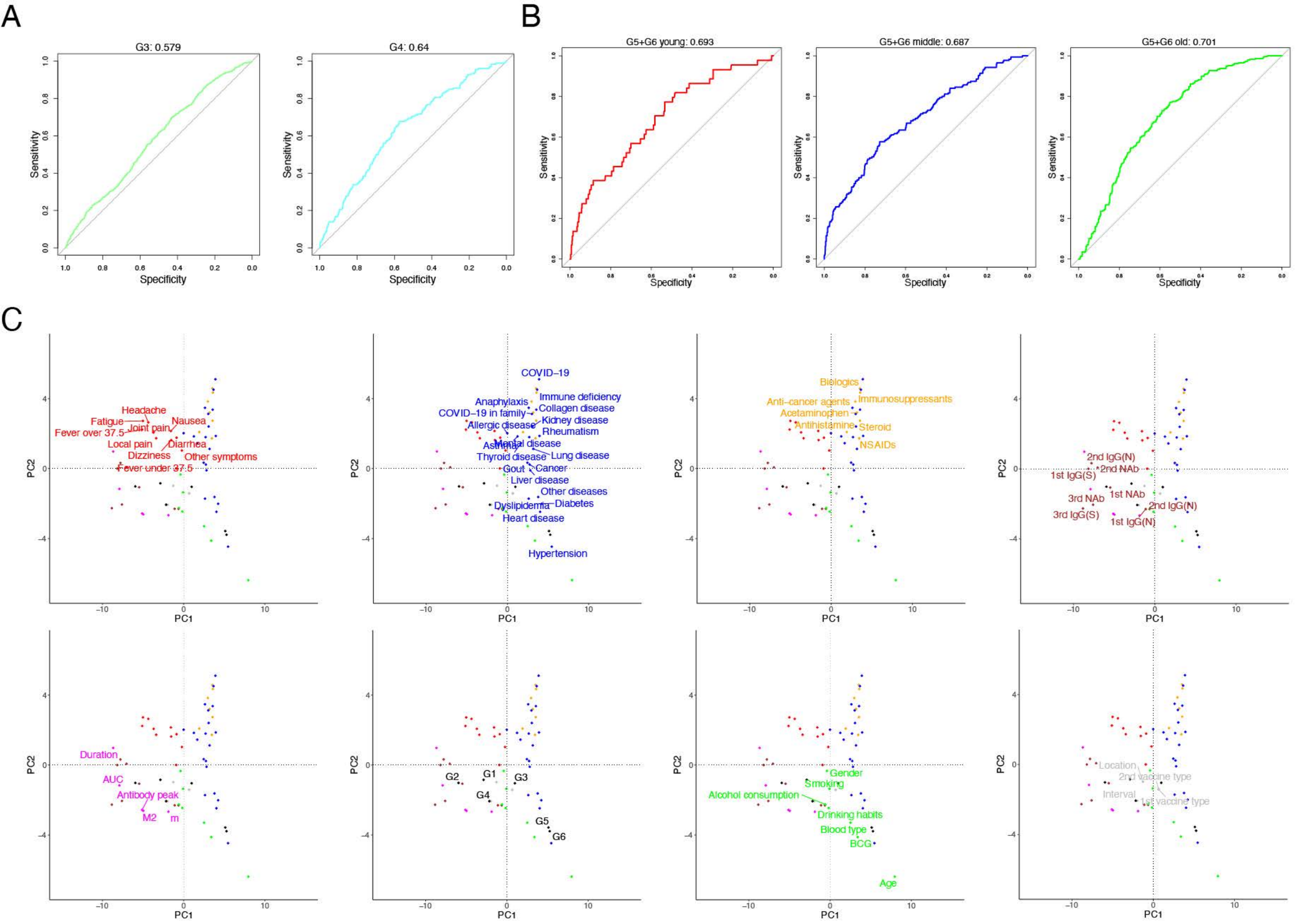
A
G3: 0.579
G4: 0.64
Sensitivity
Specificity
B
G5+G6 young: 0.693
G5+G6 middle: 0.687
G5+G6 old: 0.701
C
PC1
PC2
Headache
Fatigue
Joint pain
Nausea
Fever over 37.5
Local pain
Diarrhea
Dizziness
Other symptoms
Fever under 37.5
COVID−19
Immune deficiency
Anaphylaxis
Collagen disease
COVID−19 in family
Kidney disease
Allergic disease
Rheumatism
Asthma
Mental disease
Thyroid disease
Lung disease
Gout
Cancer
Liver disease
Other diseases
Dyslipidemia
Diabetes
Heart disease
Hypertension
Biologics
Anti−cancer agents
Immunosuppressants
Acetaminophen
Antihistamine
Steroid
NSAIDs
2nd IgG(N)
2nd NAb
1st IgG(S)
3rd NAb
1st NAb
2nd IgG(N)
3rd IgG(S)
1st IgG(N)
Duration
AUC
Antibody peak
M2
m
G2
G1
G3
G4
G5
G6
Gender
Smoking
Alcohol consumption
Drinking habits
Blood type
BCG
Age
Location
2nd vaccine type
Interval
1st vaccine type

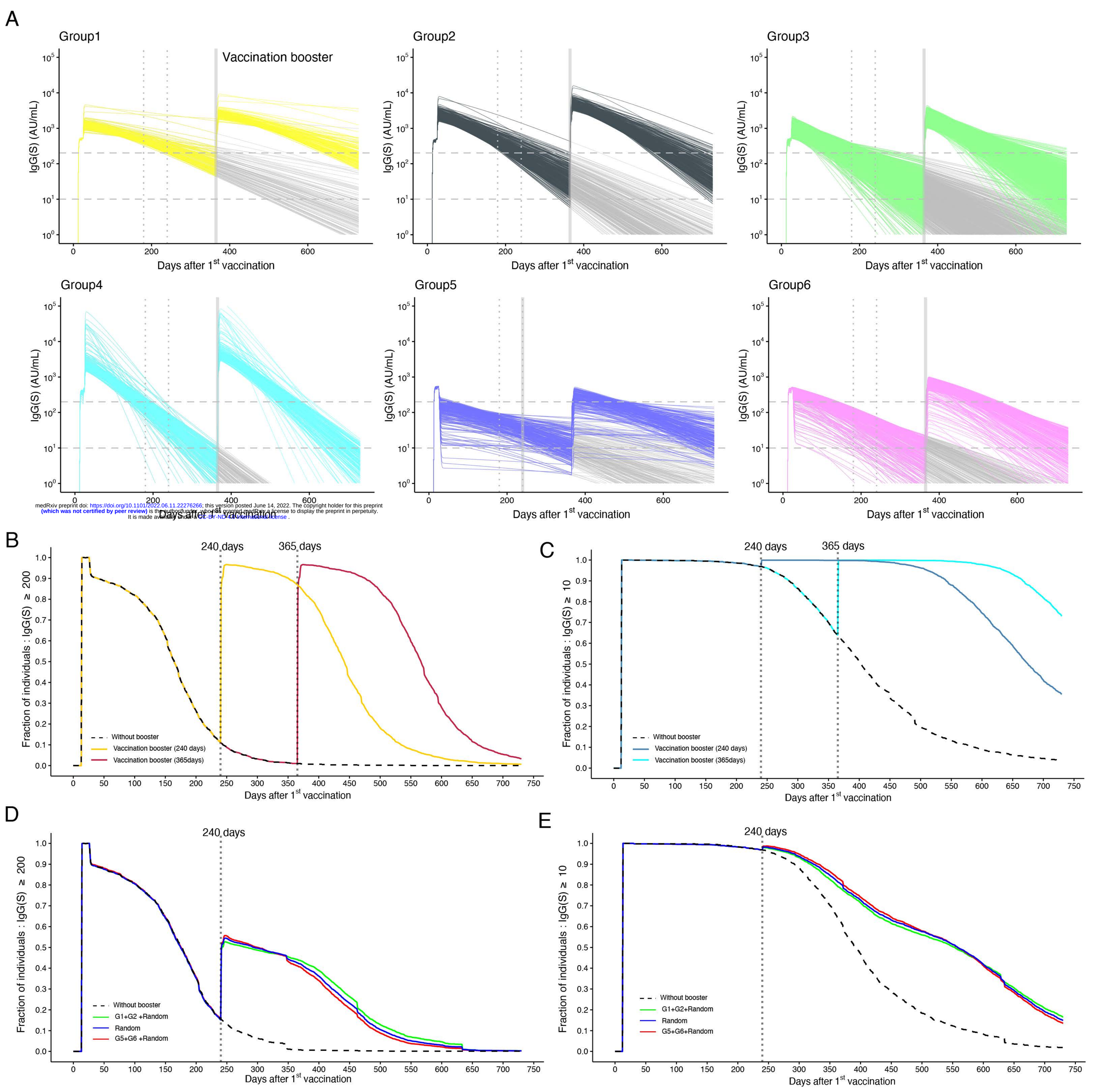

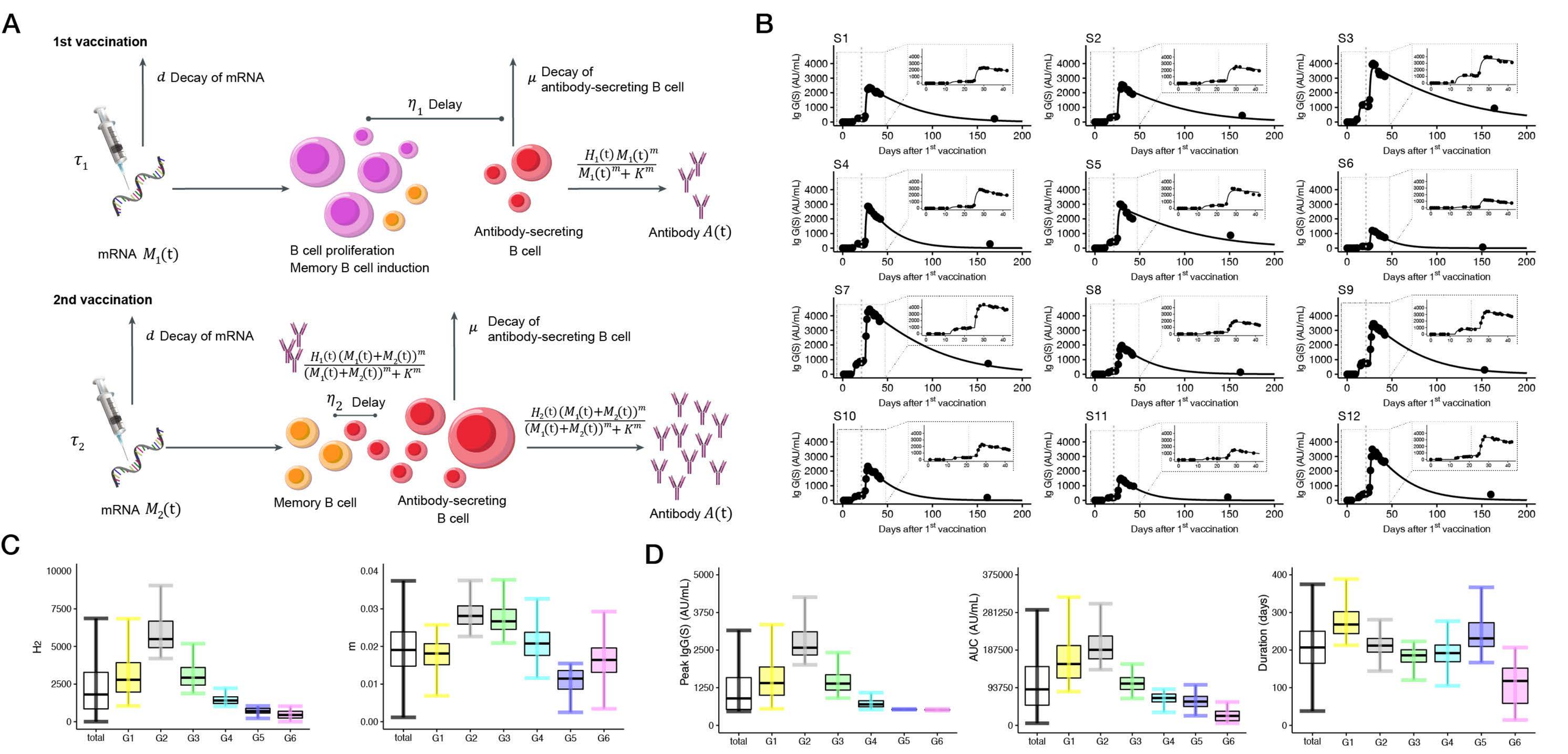
A
1st vaccination
d Decay of mRNA
η1 Delay
μ Decay of antibody-secreting B cell
τ1
mRNA M1(t)
B cell proliferation
Memory B cell induction
Antibody-secreting B cell
Antibody A(t)
2nd vaccination
d Decay of mRNA
μ Decay of antibody-secreting B cell
η2 Delay
τ2
mRNA M2(t)
Memory B cell
Antibody-secreting B cell
Antibody A(t)
B
S1
S2
S3
S4
S5
S6
S7
S8
S9
S10
S11
S12
lg G(S) (AU/mL)
Days after 1st vaccination
C
H2
m
D
Peak IgG(S) (AU/mL)
AUC (AU/mL)
Duration (days)
total
G1
G2
G3
G4
G5
G6